Journal of Mathematical Modeling and Fractional Calculus
https://acspublisher.com/journals/index.php/jmmfc
Received:21-10-2025, **Revised:** 23-11-2025,
Accepted: 17-12-2025, **Published:** 30-12-2025,
https://doi.org/10.48165/jmmfc.2025.2205, 2(2),62-99.

Control of Marburg Virus Disease Spread in Humans under Hypersensitive Response through Fractal-Fractional

Ankita Dwivedi[a], Santosh Verma[a]

[a]Guru Ghasidas Vishwavidyalaya (A Central University)Bilaspur - 495009, India.
Corresponding author Email: ankitadwivedi910@gmail.com.

Abstract:

In this study, we propose and analyze a novel fractional-order preypredator-super predator model that incorporates maturation delay, harvesting, and the Allee effect. The prey population is assumed to grow logistically under the influence of a strong Allee effect, with a time delay accounting for the maturation period. Predators and super predators interact through predation and competition, while also experiencing harvesting impacts. The system is described using the Caputo fractional derivative to better capture memory effects inherent in ecological processes. Furthermore, herd behavior in predation is represented through a generalized functional response dependent on a parameter α, modeling various herd structures such as circular, square, cubic, and spherical formations. Key parameters include the intrinsic growth rate of prey, carrying capacity, mortality rates, predation coefficients, Allee threshold, and harvesting intensities. We investigate the existence and local stability of equilibria, derive the net reproduction numbers for both predator and super predator populations, and perform a Hopf bifurcation analysis to explore the emergence of delay-induced periodic solutions. The results enhance the understanding of how memory, delay, harvesting, and Allee effects collectively influence the dynamics of ecological systems. The AdamsBashforthMoulton method is employed to approximate the solutions of the proposed model. Using Python, we perform graphical illustrations and numerical simulations to support our analysis.

Keywords: Caputo- fractional derivative; Preypredator-super predator model; Delay; Harvesting; Allee effect;

1. Introduction

The study of multi-trophic interactions, particularly predatorpreysuper predator systems, has long been a cornerstone of ecological modeling. Over time, classical models have evolved significantly to accommodate real-world complexities such as nonlinear harvesting, Allee effects, fear responses, maturation delays, and fractional-order dynamics. These extensions aim to better capture the intrinsic biological phenomena that traditional integer-order models tend to oversimplify.

The impact of nonlinear harvesting on population dynamics has attracted considerable attention. Mortuja et al. [26] analyzed a predatorprey system with a square-root functional response and nonlinear prey harvesting, uncovering rich dynamical behaviors, including multiple equilibria and bifurcations. Bhunia et al. [4] further explored the explicit influence of harvesting strategies in delayed prey predator models, emphasizing their role in determining species persistence or extinction.

Incorporating Allee effects into ecological models is critical, particularly in scenarios where low population densities may drive species toward extinction. Ma et al. [22] investigated the role of strong Allee effects in prey predator systems and demonstrated their potential to induce extinction and generate complex dynamics. Similarly, Kumar et al. [18] studied a fractional-order prey-predator model considering Allee effects, fear factors, and interspecies rivalry, highlighting the significant impact these factors have on stability and bifurcation structures.

Fractional calculus has emerged as a robust framework for modeling biological systems that exhibit memory and hereditary properties. Traditional differential equations often fail to capture these long-term memory effects, whereas fractional derivatives are well-suited for this purpose. Angstmann et al. [1] introduced a fractional-order infectivity SIR model, illustrating the value of fractional calculus in epidemiological modeling. Dwivedi and Verma [11] developed a fear-affected fractional predatorprey model with disease transmission, while Yavuz and Sene [39] demonstrated the benefits of fractional modeling in stability analysis under harvesting conditions. Furthermore, Ramesh et al. [33] emphasized the importance of time delays in fractional-order predatorprey systems and their influence on complex dynamics.

The interplay between harvesting and fractional-order dynamics has also been actively studied. Brahim et al. [7] investigated a three-species fractional predatorprey model under harvesting, revealing novel stability and bifurcation phenomena. Mukherjee et al. [27] explored optimal harvesting strategies in ecosystems with toxic prey and environmental uncertainty, while Paul et al. [31] examined the effects of fear and fractional dynamics on tri-trophic food chains.

Motivated by these advancements, we propose and analyze a novel fractional-order preypredatorsuper predator model that incorporates nonlinear harvesting, a strong Allee effect, and maturation delay. The prey population is modeled using a logistic growth law modified by a strong Allee effect and a discrete maturation delay, while predator and super predator populations are subject to harvesting and interspecific predation. To capture memory effects, we employ the Caputo fractional derivative [32, 17, 9]. Our goal is to rigorously investigate the existence and local stability of equilibria, derive reproduction numbers, analyze the onset of Hopf bifurcations induced by delay, and validate the theoretical results through numerical simulations using the AdamsBashforthMoulton method [10, 14].

1.1. Motivation

Ecological systems are inherently memory-dependent and often exhibit delayed responses due to biological processes such as gestation, maturation, and environmental feedback. Classical integer-order models frequently fail to capture such delayed memory effects accurately. Inspired by the growing body of research highlighting the importance of memory and delay in ecological dynamics, we develop a fractional-order model utilizing the Caputo derivative [32, 17, 25]. Furthermore, we incorporate nonlinear harvesting, strong Allee effects, and herd behavior to enhance the ecological realism of the model. This comprehensive framework not only extends the current understanding of ecological systems but also provides a robust tool for analyzing critical thresholds and stability under various ecological pressures.

1.2. Novelties and Contributions

The main novelties and contributions of this study are summarized below:

- **Development of a New Model:** A novel fractional-order preypredatorsuper predator model is proposed, incorporating nonlinear harvesting, a strong Allee effect, maturation delay, and herd behavior.
- **Incorporation of Memory Effects:** The Caputo fractional derivative is employed to capture the intrinsic memory effects present in biological interactions [9].
- **Generalized Functional Response:** A generalized functional response, characterized by a group structure parameter α, is introduced to model different herd predation behaviors.

- **Dual Harvesting Strategy:** Harvesting is considered simultaneously for both predator and super predator populations, offering a broader perspective for ecological management.

- **Analytical Results:** Rigorous analysis is conducted to establish the existence and local stability conditions of equilibria, and reproduction numbers are derived using the next-generation matrix method [8].

- **Bifurcation Analysis:** Hopf bifurcation induced by maturation delay is analyzed, providing insights into the emergence of periodic oscillations.

- **Numerical Validation:** Extensive numerical simulations are carried out using the AdamsBashforthMoulton scheme [10, 14], implemented in Python, to validate the theoretical findings and explore complex dynamical behaviors.

1.3. Structure of the paper

This paper is arranged as follows: We discuss some importants definations and characteristics of fractional derivatives related to this article Section 2.Preliminaries, in Section 3. Model formation,Section 4. Analysis of the model, Section 5. Analysis of Individual Equations, Section 6. Stability Analysis, Section 7. Hopf Bifuraction Criterion, Section 8. Net Reproduction Number, Section 9. Quantitative Bionomic Analysis of a Fractional Prey-Predator-Super Predator Model with Harvesting and Delay, Section 10. Optimal Harvesting Strategy for a Fractional-Order PredatorPreySuper Predator Model, Section 11. Control Variables, Section 12. Herd Shape Strategy via the Exponent α, Section 13. Impact Analysis of the Allee Threshold δ_2, Section 14. Numerical Analysis and Section 15. Conclusion.

2. Preliminary

Caputo Fractional Derivative Definition

The Caputo fractional derivative of a function [21] $f(t)$ of order $\tau \in (0,1)$ is defined as:

$$\mathscr{D}_t^\tau f(t) = \frac{1}{\Gamma(1-\tau)} \int_a^t \frac{f'(s)}{(t-s)^\tau} ds, \tag{1}$$

where:

- $\mathscr{D}_t^\tau$ denotes the Caputo derivative of order τ with respect to t,
- $\Gamma(\cdot)$ is the Gamma function,
- $f'(s)$ is the standard first derivative of f,
- a is the lower limit of integration (initial time).

General Formula for Caputo Derivative

For $\tau > 0$ with $n-1 < \tau < n$ ($n \in \mathbb{N}$), the Caputo derivative [11]is given by:

$$\mathscr{D}_t^\tau f(t) = \frac{1}{\Gamma(n-\tau)} \int_a^t \frac{f^{(n)}(s)}{(t-s)^{\tau-n+1}} ds, \tag{2}$$

where $f^{(n)}(s)$ is the n-th classical derivative of f.

Lemma 1. Let $0 < \alpha \leq 1$, and suppose that $u(t) \in C[a,b]$ with $D_C^\alpha u(t)$ continuous on $[a,b]$. Then, for any $t \in (a,b]$, there exists $\eta \in [a,t]$ such that

$$u(t) = u(a) + \frac{(t-a)^\alpha}{\Gamma(\alpha+1)} D_C^\alpha u(\eta). \tag{3}$$

Remark 1. If $D_C^\alpha u(t) \geq 0$ (respectively, $D_C^\alpha u(t) \leq 0$) for all $t \in (a,b)$, then $u(t)$ is a non-decreasing (respectively, non-increasing) function on $[a,b]$.

Lemma 2. Consider the fractional-order system

$$D_C^\alpha(Z(t)) = \Psi(Z), \tag{4}$$

with the initial condition

$$Z(t_0) = (z_1(t_0), z_2(t_0), \ldots, z_n(t_0)), \tag{5}$$

where $0 < \alpha < 1$, $Z(t) = (z_1(t), z_2(t), \ldots, z_n(t))$, and $\Psi : [t_0, \infty) \to \mathbb{R}^n$.

The equilibrium points are determined by solving $\Psi(Z) = 0$. An equilibrium point is locally asymptotically stable if each eigenvalue λ_j of the Jacobian matrix

$$M(Z) = \frac{\partial(\Psi_1, \Psi_2, \ldots, \Psi_n)}{\partial(z_1, z_2, \ldots, z_n)} \tag{6}$$

evaluated at the equilibrium satisfies

$$|\arg(\lambda_j)| > \frac{\alpha\pi}{2}. \tag{7}$$

Lemma 3. Assume that $u(t) \in \mathbb{R}^+$ is a differentiable function. Then, for all $t > 0$,

$$D_C^\alpha \left[u(t) - u^* - u^* \ln\left(\frac{u(t)}{u^*}\right) \right] \leq \left(1 - \frac{u^*}{u(t)}\right) D_C^\alpha(u(t)), \tag{8}$$

where $u^* \in \mathbb{R}^+$ and $\alpha \in (0,1)$.

3. Model formulation

In this study, we develop a fractional-order predatorpreysuper predator model that incorporates time delay, harvesting, and the Allee effect. Additionally, the model captures different herd behavior patterns through a generalized nonlinear predation function. This model formulation are explain by the help of flow chart (1, 2). The dynamics of the populations [15] are governed by the following system of fractional-order differential equations:

$$\begin{cases} D^\tau S = \pi S\left(1 - \frac{S(t-\nu)}{\delta_1}\right)(S - \delta_2) - \xi_1 S^\alpha P - \xi_2 S^\alpha W \\ D^\tau P = \xi_1 S^\alpha P - \xi_3 PW - \psi_1 P - \mathbf{h_1} P^2 \\ D^\tau W = \xi_2 S^\alpha W - \xi_3 PW - \psi_2 W - \mathbf{h_2} W^2 \end{cases} \tag{9}$$

Step-by-Step Construction of the Model:

1. **Prey Dynamics:**
   The prey population follows logistic growth with a carrying capacity δ_1, and experiences an Allee effect with threshold δ_2. Predation by both predators and super predators is modeled through a nonlinear term proportional to S^α.
2. **Predator Dynamics:**
   The predator population increases via consumption of prey, and decreases due to natural mortality (ψ_1), intra-species competition ($\mathbf{h_1} P^2$), and predation by the super predator ($\xi_3 PW$).
3. **Super Predator Dynamics:**
   The super predator benefits from consuming both prey and predator populations. Losses occur due to natural mortality (ψ_2) and density-dependent harvesting ($\mathbf{h_2} W^2$).

4. **Fractional-Order Derivatives:**
   The use of the Caputo fractional derivative D^{τ} introduces memory effects into the system, capturing the historical influence on the current population dynamics.
5. **Incorporation of Time Delay:**
   A discrete time delay ν is included in the prey equation to represent the maturation delay between birth and adulthood, significantly affecting the prey's effective reproduction.

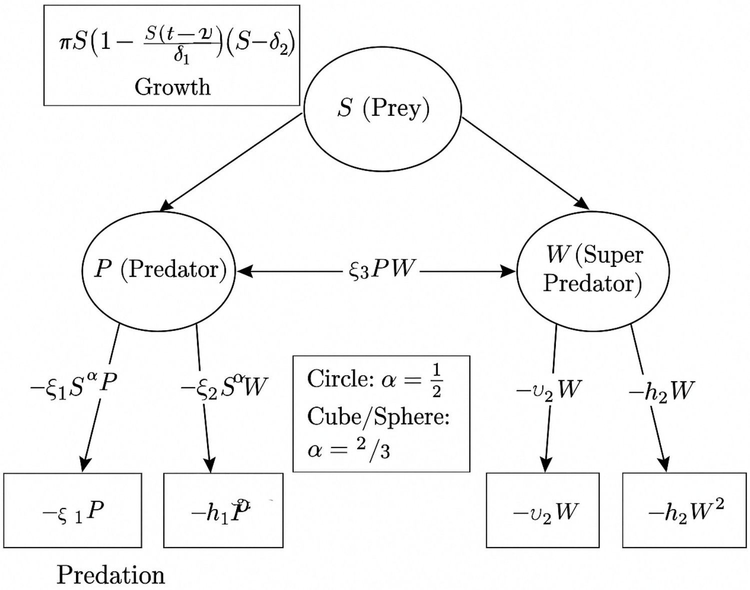

Figure 1: Flow Chart 1

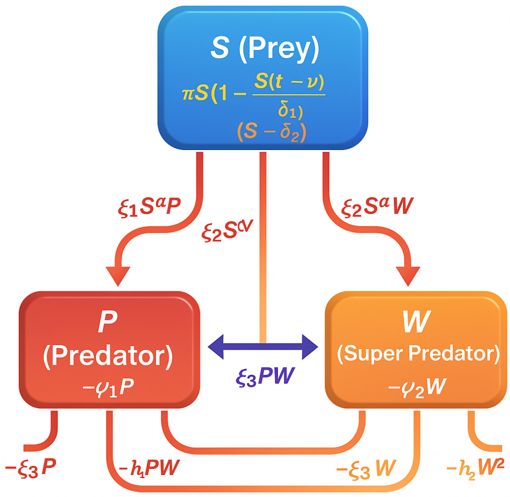

Figure 2: Flow Chart 2

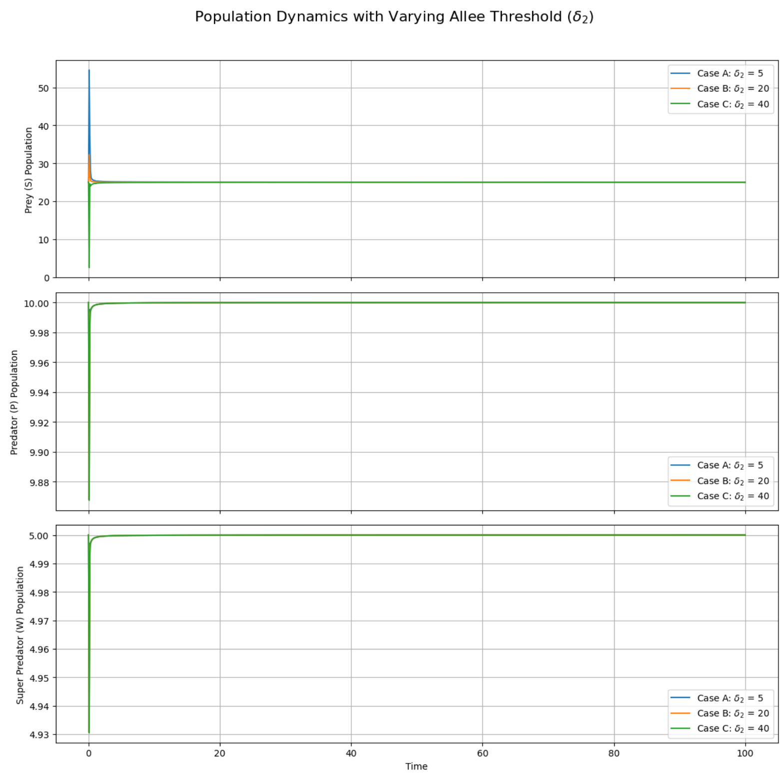

Figure 3: Population Dynamics with varying Allee Threshold

Simulation Results of the Fractional-Order Delayed Predator-Prey-Super Predator Model with Allee Effect.

Simulation Overview

The following simulation results are obtained using the Caputo fractional derivative, incorporating both the memory effect and time delay. The evolution of prey, predator, and super predator populations is analyzed under three different Allee threshold scenarios:

- **Low Allee Threshold** ($\delta_2 = 5$): The prey population grows more easily due to a weak Allee effect.
- **Moderate Allee Threshold** ($\delta_2 = 20$): The prey experiences moderate difficulty in sustaining its population.
- **High Allee Threshold** ($\delta_2 = 40$): A strong Allee effect significantly impedes the prey's ability to survive and grow.

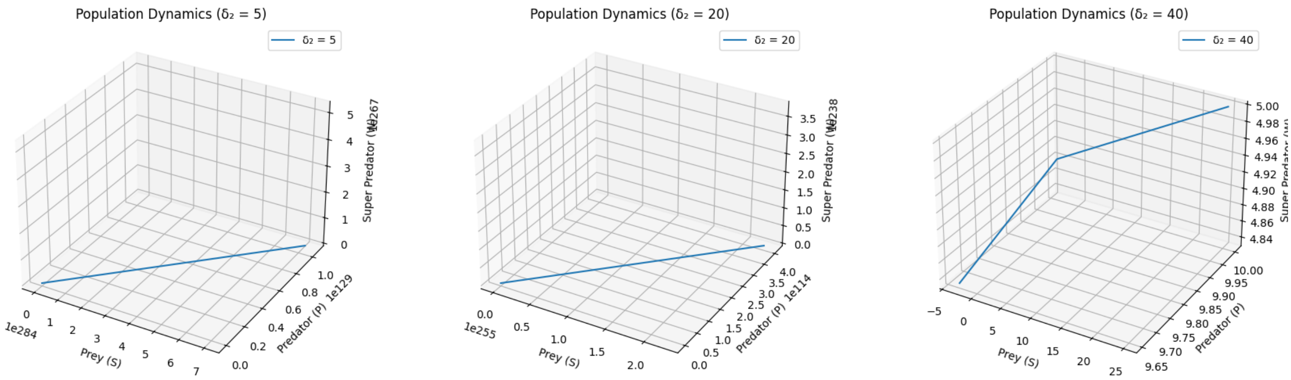

Figure 4: 3D trajectories of the prey (S), predator (P), and super predator (W) populations over time, for varying values of the Allee threshold parameter δ_2, under a fractional-order Caputo derivative model with time delay.

- **Case A** ($\delta_2 = 5$): Low threshold
- **Case B** ($\delta_2 = 20$): Moderate threshold
- **Case C** ($\delta_2 = 40$): High threshold

Each trajectory demonstrates how the population levels of the three species evolve and interact over time. The nonlinear feedback loops and delayed response mechanisms influence the amplitude and periodicity of oscillations.
Observations:

- **Case A**, with a low Allee threshold, populations remain bounded and exhibit sustained oscillatory dynamics.
- **Case B**, increasing δ_2 causes moderate destabilization and amplifies the amplitude of oscillations.
- **Case C**, the high Allee threshold introduces stronger feedback effects, leading to population spikes or collapses. Numerical instabilities may arise due to overflow or excessively rapid growth.

These behaviors underscore the importance of the Allee effect in shaping the long-term dynamics of ecological systems, especially under fractional-order memory and time-delay influences.

4. Analysis of the model

This section investigates the existence, uniqueness, non-negativity, and boundedness of the proposed model.

4.1. Existence and Uniqueness

Theorem 4.1. *There exists a unique solution of the proposed model* (9) *for each non-negative condition.*

Proof. We are seeking for a sufficient condition for the presence and uniqueness of the proposed model (9) solutions in the region $\theta \times [0,T]$, where $\theta = (S,P,W) \in \mathbb{R}^3 : \max ||S||, ||P||, ||W||$. The method employed is used consider a mapping: $H(Y) = H_1(Y), H_2(Y), H_3(Y)$ where $Y = (S, P, W)$ and $\hat{Y} = (\hat{S}, \hat{P}, \hat{W})$

$$\begin{cases} H_1(Y) = \pi S\left(1-\frac{S(t-\nu)}{\delta_1}\right)(S-\delta_2) - \xi_1 S^{\alpha} P - \xi_2 S^{\alpha} W \\ H_2(Y) = \xi_1 S^{\alpha} P - \xi_3 PW - \psi_1 P - \mathbf{h_1} P^2 \\ H_3(Y) = \xi_2 S^{\alpha} W - \xi_3 PW - \psi_2 W - \mathbf{h_2} W^2 \\ ||H(Y) - H(\hat{Y})|| = |H_1(Y) - H_1(\hat{Y})| + |H_2(Y) - H_2(\hat{Y})| + |H_3(Y) - H_3(\hat{Y})| \\ = \bigg|\left(\pi S\left(1-\frac{S(t-\nu)}{\delta_1}\right)(S-\delta_2) - \xi_1 S^{\alpha} P - \xi_2 S^{\alpha} W\right) - \left(\pi \hat{S}\left(1-\frac{\hat{S}(t-\nu)}{\delta_1}\right)(\hat{S}-\delta_2) - \xi_1 \hat{S}^{\alpha} \hat{P} - \xi_2 \hat{S}^{\alpha} \hat{W}\right)\bigg| \\ + \big|(\xi_1 S^{\alpha} P - \xi_3 PW - \psi_1 P - \mathbf{h_1} P^2) - (\xi_1 \hat{S}^{\alpha} \hat{P} - \xi_3 \hat{P}\hat{W} - \psi_1 \hat{P} - \mathbf{h_1} P^2)\big| \\ + \big|(\xi_2 S^{\alpha} W - \xi_3 PW - \psi_2 W - \mathbf{h_2} W^2) - (\xi_2 \hat{S}^{\alpha} \hat{W} - \xi_3 \hat{P}\hat{W} - \psi_2 \hat{W} - \mathbf{h_2} \hat{W}^2)\big| \\ = \pi\delta_1|S+\hat{S}||S-\hat{S}| - \pi(t^2-\nu)|S+\hat{S}||S^2 - S\hat{S} + \hat{S}^2| + \delta_2\delta_1(t-\nu)|S-\hat{S}| \\ -2\xi_2|PW - \hat{P}\hat{W}| - \psi_1|P-\hat{P}| - \mathbf{h_1}|P+\hat{P}||P-\hat{P}| - \psi_2|W-\hat{W}| - \mathbf{h_2}|W+\hat{W}||W-\hat{W}| \\ = \pi\delta_1|S+\hat{S}||S-\hat{S}| - \pi(t^2-\nu)|S-\hat{S}||S^2 - S\hat{S} + \hat{S}^2 + \delta_2\delta_1(t-\nu)|S-\hat{S}| - 2\xi_2\delta_1|PW \\ -\hat{P}\hat{W}| - \delta_1^2\psi_1|P-\hat{P}| - \delta_1^2\mathbf{h_1}|P+\hat{P}||P-\hat{P}| - \delta_1^2\psi_2|W-\hat{W} - \delta_1^2\mathbf{h_2}|W+\hat{W}||W-\hat{W}| \\ \leq \delta_2\delta_1(t-\nu)|S-\hat{S}| - \delta_1^2\psi_1|P-\hat{P}| - \psi_2\delta_1^2|W-\hat{W}| + \pi\delta_1|S+\hat{S}||S-\hat{S}| - \pi(t^2-\nu)|S+\hat{S}||S^2 \\ -S\hat{S} + \hat{S}^2 - 2\xi_2\delta_1^2|PW - \hat{P}\hat{W}| - \delta_1\mathbf{h_1}|P+\hat{P}| - \delta_1^2\mathbf{h_2}|W+\hat{W}||W-\hat{W}| \\ \leq \frac{(2\pi\delta_1 M + \delta_2\delta_1(t-\nu))|S-\hat{S}| - \pi(t^2-\nu)|S-\hat{S}||S^2 - S\hat{S} + \hat{S}^2|}{\delta_1^2}(\xi_1 S^{\alpha} - \psi)|W-\hat{W} - \xi_3|PW - \hat{P}\hat{W}| \\ +2M|W-\hat{W}| + \xi_1|S^{\alpha}P - \hat{S}^{\alpha}\hat{P}| - \xi_3|PW - \hat{P}\hat{W}| - \psi_1|P-\hat{P}| + 2M\mathbf{h_1}|P-\hat{P}| \\ -\xi_1|S^{\alpha}P - \hat{S}^{\alpha}\hat{P}| - \xi_2|S^{\alpha}W - \hat{S}^{\alpha}\hat{W}| \\ \leq H_1|S-\hat{S}| + H_2|P-\hat{P}| + H_3|W-\hat{W}| \\ \leq H||Y-\hat{Y}|| \end{cases} \tag{10}$$

where $H = \max H_1, H_2, H_3$

As a result $H(Y)$ satisfies the lipschitz condition, ensuring the existence and uniqueness of the fractional order system (9). □

5. Analysis of Individual Equations

To understand the system's behavior, we analyze each equation separately.

Prey Population Dynamics The prey population follows:

$$D^{\tau}S = \pi S\left(1-\frac{S(t-\nu)}{\delta_1}\right)(S-\delta_2) - \xi_1 S^{\alpha} P - \xi_2 S^{\alpha} W. \tag{11}$$

This represents logistic growth with an Allee effect and predation.

Predator Population Dynamics The predator population equation is:

$$D^{\tau}P = \xi_1 S^{\alpha} P - \xi_3 PW - \psi_1 P - \mathbf{h_1} P^2. \tag{12}$$

This describes predator growth through prey consumption, natural death, and harvesting.

Super Predator Population Dynamics The super predator follows:

$$D^{\tau}W = \xi_2 S^{\alpha} W - \xi_3 PW - \psi_2 W - \mathbf{h_2} W^2. \tag{13}$$

This equation accounts for super predator growth based on prey and predator consumption, along with natural mortality and harvesting. S= Prey Population
P= Predator Population

W= Super Predator Population
π= increasing rate of prey population
ψ_1= Natural death rate for predator population
ψ_2= Natural death rate for super predator population
δ_1= Carrying capacity of prey population
δ_2= Allee threshold effect
ξ_1, ξ_2 = Predation rate for the predator(Super predator on the prey)
ξ_3= Predation rate of the super predator on a predator
α= rate of herd shape[Circle, Square, Cube and Sphere][Circle herd shape α takes the value$\frac{1}{2}$ and for the cube and sphere herd shape the rate α atkes the values $\frac{2}{3}$]
ν= unit of the taken by newborn to become adult at the present time
$\mathbf{h}_1$= Harvesting on Predator.
$\mathbf{h}_2$= Harvesting on super Predator.

6. Stability Analysis

In this part we will identify all of system (9)'s trivial and non-trivial equilibruim points as well as their existence conditions [16, 36].

6.1. *Equilibrium Points and Existence Criteria of the System:*

There are five different types of equilibrium points in system.

Equilibrium Equations To find the equilibrium points, we set the time derivatives to zero: To determine the equilibrium points of the system, we set the right-hand sides of the equations to zero:

$$\begin{cases} D^{\tau}S &= \pi S\left(1-\frac{S(t-\nu)}{\delta_1}\right)(S-\delta_2)-\xi_1 S^{\alpha}P-\xi_2 S^{\alpha}W=0, \\ D^{\tau}P &= \xi_1 S^{\alpha}P-\xi_3 PW-\psi_1 P-\mathbf{h_1}P^2=0, \\ D^{\tau}W &= \xi_2 S^{\alpha}W-\xi_3 PW-\psi_2 W-\mathbf{h_2}W^2=0. \end{cases} \tag{14}$$

1. Trivial Equilibrium Point Setting $S=0$, $P=0$, and $W=0$, we obtain:

$$E_0=(0,0,0). \tag{15}$$

2. Axial equilibrium Predator and Super Predator Absent. For equilibrium $E_1=(S_1,0,0)$, setting $P=0$ and $W=0$, we solve for S_1:

$$\pi S\left(1-\frac{S}{\delta_1}\right)(S-\delta_2)=0. \tag{16}$$

Solving for S gives:

$$S=0, \quad S=\delta_1, \quad S=\delta_2. \tag{17}$$

Thus, the possible equilibrium points are:

$$E_1=(\delta_2,0,0) \quad \text{and} \quad E_1=(\delta_1,0,0). \tag{18}$$

provided they are biologically meaningful.

3. Planar Equilibrium Predator Absent, Super Predator Present. For equilibrium $E_2=(S_2,0,W_2)$, setting $P=0$ and solving:

$$\pi S\left(1-\frac{S}{\delta_1}\right)(S-\delta_2)-\xi_2 S^{\alpha}W=0. \tag{19}$$

$$\xi_2 S^{\alpha}W-\psi_2 W-\mathbf{h_2}W^2=0. \tag{20}$$

From the second equation:

$$W(\xi_2 S^{\alpha} - \psi_2 - \mathbf{h_2} W) = 0. \tag{21}$$

Solving for W:

$$W = 0 \quad \text{or} \quad W = \frac{\xi_2 S^{\alpha} - \psi_2}{\mathbf{h_2}}. \tag{22}$$

Substituting this into the 19 equation determines S. We are given the following two equations:

Well substitute both values of W into Equation 19 separately to find corresponding values of S.

Case 1: $W = 0$ Substitute into Equation 19: This gives a product of three terms, so the solutions are:

$$S = 0, \quad S = \delta_1, \quad S = \delta_2 \tag{23}$$

Case 2: $W = \frac{\xi_2 S^{\alpha} - \psi_2}{\mathbf{h_2}}$
Substitute into Equation 19:

$$\pi S\left(1 - \frac{S}{\delta_1}\right)(S - \delta_2) - \xi_2 S^{\alpha}\left(\frac{\xi_2 S^{\alpha} - \psi_2}{\mathbf{h_2}}\right) = 0 \tag{24}$$

Multiply out the second term:

$$\pi S\left(1 - \frac{S}{\delta_1}\right)(S - \delta_2) - \frac{\xi_2^2 S^{2\alpha} - \xi_2 \psi_2 S^{\alpha}}{\mathbf{h_2}} = 0 \tag{25}$$

Multiply through by $\mathbf{h_2}$ to eliminate the denominator:

$$\mathbf{h_2}\pi S\left(1 - \frac{S}{\delta_1}\right)(S - \delta_2) - \xi_2^2 S^{2\alpha} + \xi_2 \psi_2 S^{\alpha} = 0 \tag{26}$$

This is now an algebraic equation in terms of S, which may be solved either symbolically or numerically.

$$-\frac{\mathbf{h_2}\pi}{\delta_1}x^6 + \mathbf{h_2}\pi\left(1 + \frac{\delta_2}{\delta_1}\right)x^4 - \left(\mathbf{h_2}\pi\delta_2 + \xi_2^2\right)x^2 + \xi_2\psi_2 x = 0 \tag{27}$$

4. Planar equilibrium points Predator Present, Super Predator Absent For equilibrium $E_3 = (S_3, P_3, 0)$, setting $W = 0$ and solving:

$$\pi S\left(1 - \frac{S_3}{\delta_1}\right)(S - \delta_2) - \xi_1 S^{\alpha} P = 0. \tag{28}$$

$$\xi_1 S^{\alpha} P - \psi_1 P - \mathbf{h_1} P^2 = 0. \tag{29}$$

from the second equation:

$$P(\xi_1 S^{\alpha} - \psi_1 - \mathbf{h_1} P) = 0. \tag{30}$$

solving for P:

$$P = 0 \quad \text{or} \quad P = \frac{\xi_1 S^{\alpha} - \psi_1}{\mathbf{h_1}}. \tag{31}$$

Substituting this into the first equation (28) determines S. We are given:

Case 1: $P = 0$

$$\pi S\left(1 - \frac{S_3}{\delta_1}\right)(S - \delta_2) = 0 \tag{32}$$

Thus, the solutions are:

$$S = 0 \quad \text{or} \quad S = \delta_2$$

Case 2: $P = \frac{\xi_1 S^\alpha - \psi_1}{\mathbf{h_1}}$
Substitute into Equation (1):

$$\pi S\left(1-\frac{S_3}{\delta_1}\right)(S-\delta_2)-\xi_1 S^\alpha\left(\frac{\xi_1 S^\alpha-\psi_1}{\mathbf{h_1}}\right)=0 \tag{33}$$

Simplify:

$$\pi S\left(1-\frac{S_3}{\delta_1}\right)(S-\delta_2)-\frac{\xi_1^2 S^{2\alpha}-\xi_1\psi_1 S^\alpha}{\mathbf{h_1}}=0 \tag{34}$$

Multiply through by $\mathbf{h_1}$:

$$\mathbf{h_1}\pi S\left(1-\frac{S_3}{\delta_1}\right)(S-\delta_2)-\xi_1^2 S^{2\alpha}+\xi_1\psi_1 S^\alpha=0 \tag{35}$$

6.2. Local Stability Analysis

The Jacobian matrix of the model (9) at (S, P, W) can be represent as

$$J(S,P,W)=\begin{bmatrix}\frac{\partial f_1}{\partial S} & \frac{\partial f_1}{\partial P} & \frac{\partial f_1}{\partial W}\\ \frac{\partial f_2}{\partial S} & \frac{\partial f_2}{\partial P} & \frac{\partial f_2}{\partial W}\\ \frac{\partial f_3}{\partial S} & \frac{\partial f_3}{\partial P} & \frac{\partial f_3}{\partial W}\end{bmatrix}, \tag{36}$$

where we computing the partial derivatives:

$$\begin{aligned}
&\frac{\partial f_1}{\partial S}=\pi\left[\left(1-\frac{2S}{\delta_1}\right)(S-\delta_2)+S\left(1-\frac{S}{\delta_1}\right)\right]-\alpha\xi_1 S^{\alpha-1}P-\alpha\xi_2 S^{\alpha-1}W,\\
&\frac{\partial f_1}{\partial P}=-\xi_1 S^\alpha, \quad \frac{\partial f_1}{\partial W}=-\xi_2 S^\alpha,\\
&\frac{\partial f_2}{\partial S}=\alpha\xi_1 S^{\alpha-1}P,\\
&\frac{\partial f_2}{\partial P}=\xi_1 S^\alpha-\xi_3 W-\psi_1-2\mathbf{h_1}P, \quad \frac{\partial f_2}{\partial W}=-\xi_3 P,\\
&\frac{\partial f_3}{\partial S}=\alpha\xi_2 S^{\alpha-1}W,\\
&\frac{\partial f_3}{\partial P}=-\xi_3 W, \quad \frac{\partial f_3}{\partial W}=\xi_2 S^\alpha-\xi_3 P-\psi_2-2\mathbf{h_2}W.
\end{aligned}$$

Theorem 6.1. *The local stability of the equilibrium* $E_0=(0,0,0)$ *system*(9) *always exihits unstable behavior at* $E_0=(0,0,0)$.

Proof. The eigenvalues of the Jacobian matrix while computing Partial Derivatives at $E_0=(0,0,0)$. Evaluating the Jacobian at $(0,0,0)$:

$$J(0,0,0)=\begin{bmatrix}\pi(1-0)(0-\delta_2) & -\xi_1\cdot 0^\alpha & -\xi_2\cdot 0^\alpha\\ 0 & -\psi_1 & 0\\ 0 & 0 & -\psi_2\end{bmatrix}. \tag{37}$$

simplifying,

$$J(0,0,0)=\begin{bmatrix}-\pi\delta_2 & 0 & 0\\ 0 & -\psi_1 & 0\\ 0 & 0 & -\psi_2\end{bmatrix}. \tag{38}$$

Compute Eigenvalues: Since $J(0,0,0)$ is a diagonal matrix, its eigenvalues are simply the diagonal elements:

$$\lambda_1 = -\pi\delta_2, \quad \lambda_2 = -\psi_1, \quad \lambda_3 = -\psi_2. \tag{39}$$

then we do stability Analysis for E_0 to be locally stable, all eigenvalues must have negative real parts. Since:

- $-\pi\delta_2 < 0$ (assuming $\pi, \delta_2 > 0$),
- $-\psi_1 < 0$ (assuming $\psi_1 > 0$),
- $-\psi_2 < 0$ (assuming $\psi_2 > 0$),

all eigenvalues are negative, implying that E_0 is locally stable. □

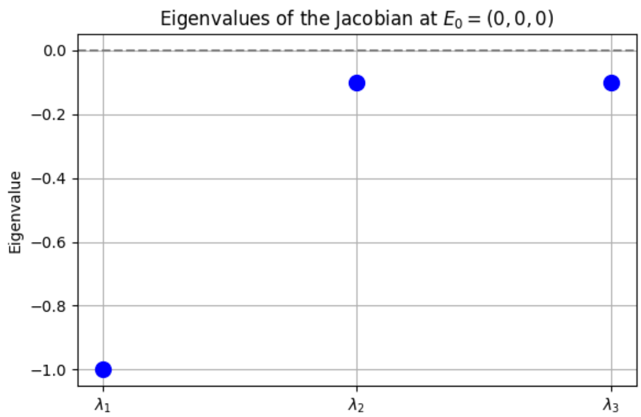

Figure 5: The equilibrium point $E_0 = (0,0,0)$

Since all eigenvalues have negative real parts, the equilibrium point E_0 is **locally asymptotically stable** under the given parameter values. by the help of table (3, 4).

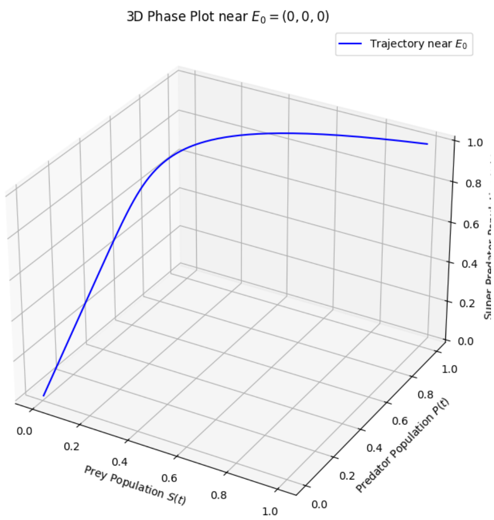

Figure 6: This show how the prey, predator, and super predator populations behave near the trivial equilibrium point $E_0 = (0,0,0)$.

As shown in Figure, the 3D phase plot illustrates how the prey, predator, and super predator populations behave near the trivial equilibrium point $E_0 = (0,0,0)$. As expected, due to all eigenvalues being negative, the system trajectories decay exponentially toward the origin, confirming the local stability of E_0.

Outcomes: The equilibrium point $E_0 = (0,0,0)$ is locally stable if the parameters π, δ_2, ψ_1, and ψ_2 are all positive by the help of table (3, 4).

Theorem 6.2. *The system of equation* (9) *is locally asymptotic stable at* $E_1 = (S_1, 0, 0)$

Proof. The system of equations governing the predator-prey-super predator model is:(9) Computing the partial derivatives:

Evaluation at $E_1 = (S_1, 0, 0)$

Substituting $P = 0$ and $W = 0$, the Jacobian matrix simplifies to a diagonal form:

$$J(E_1) = \begin{bmatrix} J_{11} & 0 & 0 \\ 0 & J_{22} & 0 \\ 0 & 0 & J_{33} \end{bmatrix}, \tag{40}$$

where:

$$\begin{aligned} J_{11} &= \pi S_1 \left(1 - \frac{S_1}{\delta_1}\right) + \pi(S_1 - \delta_2)\left(1 - \frac{S_1}{\delta_1}\right), \\ J_{22} &= \xi_1 S_1^{\alpha} - \psi_1, \\ J_{33} &= \xi_2 S_1^{\alpha} - \psi_2. \end{aligned}$$

Eigenvalues and Stability Conditions

Since the Jacobian matrix is diagonal at E_1, the eigenvalues are given by:

$$\lambda_1 = J_{11}, \quad \lambda_2 = J_{22}, \quad \lambda_3 = J_{33}. \tag{41}$$

For local stability, all eigenvalues must have negative real parts:

$$\begin{aligned} &\lambda_1 < 0 \Rightarrow \pi S_1 \left(1 - \frac{S_1}{\delta_1}\right) + \pi(S_1 - \delta_2)\left(1 - \frac{S_1}{\delta_1}\right) < 0, \\ &\lambda_2 < 0 \Rightarrow \xi_1 S_1^{\alpha} - \psi_1 < 0 \Rightarrow S_1^{\alpha} < \frac{\psi_1}{\xi_1}, \\ &\lambda_3 < 0 \Rightarrow \xi_2 S_1^{\alpha} - \psi_2 < 0 \Rightarrow S_1^{\alpha} < \frac{\psi_2}{\xi_2}. \end{aligned}$$

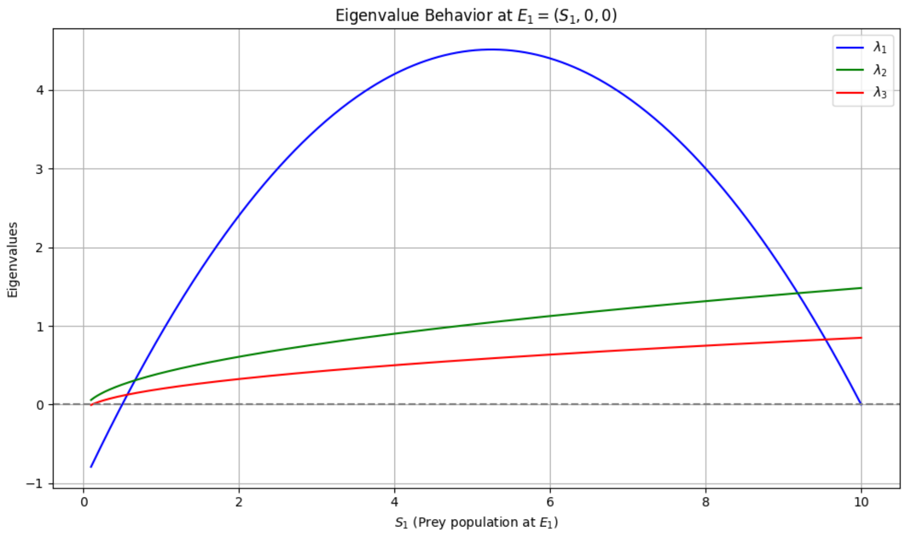

Figure 7: This shows how each eigenvalue varies with respect to the prey population S_1.

The plot below shows how each eigenvalue varies with respect to the prey population S_1. Regions where all eigenvalues are negative correspond to local asymptotic stability of E_1 by the help of table (3, 4).

Outcomes

The equilibrium point $E_1 = (S_1, 0, 0)$ is locally asymptotically stable if the following conditions hold:

$$\pi S_1 \left(1 - \frac{S_1}{\delta_1}\right) + \pi(S_1 - \delta_2)\left(1 - \frac{S_1}{\delta_1}\right) < 0,$$
$$S_1^\alpha < \frac{\psi_1}{\xi_1},$$
$$S_1^\alpha < \frac{\psi_2}{\xi_2}.$$

If any of these conditions fail, the equilibrium E_1 is either unstable or requires further analysis. □

Theorem 6.3. *The governing equations of the model system are:* (9) *is locally stable at* $E_2 = (S_2, P_2, 0)$

Proof. **Analysis of the Local Stability of the Equilibrium Point** $E_2 = (S_2, P_2, 0)$

Evaluate the Jacobian at $E_2(S_2, P_2, 0)$. Substitute $W = 0$ into the Jacobian matrix. The resulting matrix $J(E_2)$ is:

$$J(E_2) = \begin{bmatrix} J_{11} & J_{12} & J_{13} \\ J_{21} & J_{22} & J_{23} \\ J_{31} & J_{32} & J_{33} \end{bmatrix},$$

where:

$$\begin{cases} J_{11} = \pi\left(1 - \frac{S_2}{\delta_1}\right)(S_2 - \delta_2) + \pi S_2\left(1 - \frac{S_2}{\delta_1}\right) - \xi_1 \alpha S_2^{\alpha-1} P_2, \\ J_{12} = -\xi_1 S_2^\alpha, \quad J_{13} = -\xi_2 S_2^\alpha, \\ J_{21} = \xi_1 \alpha S_2^{\alpha-1} P_2, J_{22} = \xi_1 S_2^\alpha - \xi_3 W - \psi_1 - 2\mathbf{h_1} P_2, J_{23} = -\xi_3 P_2, \\ J_{31} = 0, \quad J_{32} = 0, \quad J_{33} = \xi_2 S_2^\alpha - \psi_2. \end{cases} \tag{42}$$

Compute Eigenvalues of the Jacobian matrix $J(E_2)$ are the solutions to the characteristic equation [12]:

$$\det(J - \lambda I) = 0.$$

since the Jacobian matrix $J(E_2)$ is lower triangular (with $J_{31} = J_{32} = 0$), its eigenvalues are the diagonal elements:

$$\lambda_1 = J_{11}, \quad \lambda_2 = J_{22}, \quad \lambda_3 = J_{33}.$$

for the equilibrium point E_2 to be locally stable, all eigenvalues must have negative real parts:

$$\Re(\lambda_1) < 0, \quad \Re(\lambda_2) < 0, \quad \Re(\lambda_3) < 0.$$

Since $J_{33} = \xi_2 S_2^\alpha - \psi_2$, the third eigenvalue will be negative if:

$$\xi_2 S_2^\alpha < \psi_2.$$

thus, for local stability, the following conditions must hold:

$$J_{11} < 0, \quad J_{22} < 0, \quad \xi_2 S_2^\alpha < \psi_2.$$

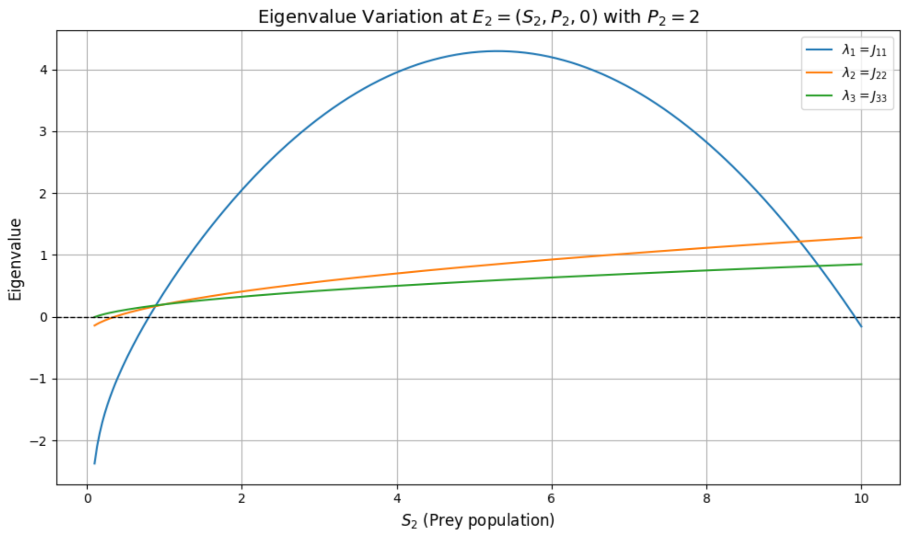

Figure 8: This graph represents the eigenvalues of the Jacobian matrix at the equilibrium point $E_2 = (S_2, P_2, 0)$

This graph represents the eigenvalues of the Jacobian matrix at the equilibrium point $E_2 = (S_2, P_2, 0)$ as a function of S_2, with $P_2 = 2$ and $W = 0$. The trends of the three eigenvalues $\lambda_1 = J_{11}$, $\lambda_2 = J_{22}$, and $\lambda_3 = J_{33}$ fig(**??**) are shown. For stability, it is necessary that all three eigenvalues have negative real parts. From the graph, one can observe the range of S_2 values for which this condition holds. If all eigenvalues are negative at a particular point, the equilibrium point E_2 is locally stable.
Outcomes: The equilibrium point $E_2 = (S_2, P_2, 0)$ is locally stable if the above conditions are satisfied. A numerical verification can be performed by explicitly calculating the eigenvalues for given parameter values by the help of table (3, 4). □

Theorem 6.4. *The equilibrium point $E_3(0, P_3, 0)$ is locally asymptotically stable under the biologically reasonable conditions $\pi, \delta_2, \psi_1, \psi_2, \xi_3, \mathbf{h_1} > 0$.*

Proof. Evaluating the Jacobian matrix at $E_3(0, P_3, 0)$ by substituting $S = 0$, $P = P_3 = \frac{\psi_1}{\mathbf{h_1}}$, and $W = 0$, we obtain:

$$J(E_3) = \begin{bmatrix} -\pi\delta_2 & 0 & 0 \\ 0 & -3\psi_1 & -\xi_3 \frac{\psi_1}{\mathbf{h_1}} \\ 0 & -\xi_3 \frac{\psi_1}{\mathbf{h_1}} & -\psi_2 \end{bmatrix}.$$

Since the Jacobian is a triangular matrix, its eigenvalues are simply the diagonal elements:

$$\lambda_1 = -\pi\delta_2, \quad \lambda_2 = -3\psi_1, \quad \lambda_3 = -\xi_3 \frac{\psi_1}{\mathbf{h_1}} - \psi_2.$$

Given that all parameters $\pi, \delta_2, \psi_1, \psi_2, \xi_3, \mathbf{h_1}$ are positive, it follows that all eigenvalues are negative. Therefore, the equilibrium point $E_3(0, P_3, 0)$ is locally asymptotically stable.
Outcomes: Let $E_3(0, P_3, 0)$ be an equilibrium point of the fractional-order predator-prey-super predator model, where $P_3 = \dfrac{\psi_1}{\mathbf{h_1}}$. Assume all parameters $\pi, \delta_2, \psi_1, \psi_2, \xi_3, \mathbf{h_1}$ are strictly positive. Then the equilibrium point E_3 is **locally asymptotically stable**.

□

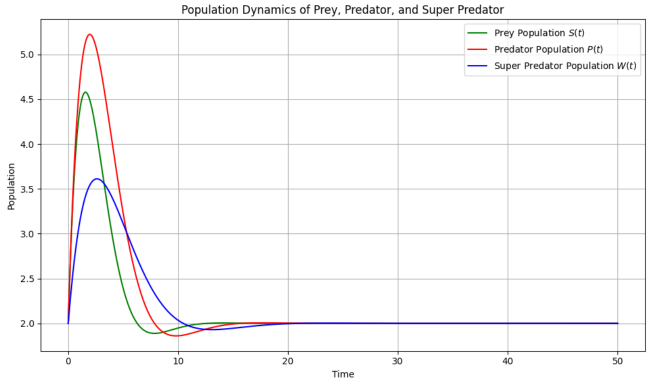

Figure 9: The equilibrium point $E_3(0, P_3, 0)$ is locally asymptotically stable

The prey population $S(t)$ initially grows by utilizing favorable environmental conditions but eventually collapses due to predation and competition. The predator population $P(t)$ closely follows the dynamics of the prey, experiencing a rise when prey is abundant and declining sharply as the prey population diminishes. Meanwhile, the super predator population $W(t)$ steadily declines over time, unable to sustain itself in the absence of sufficient predator biomass by the help of table (3, 4).

Theorem 6.5. *Local asymptotic stability of the equilibrium point* $E_4 = (S_4, 0, W_4)$.

Proof. Consider the delayed fractional-order prey-predator-super predator model with Allee effect and harvesting. The equilibrium point $E_4 = (S_4, 0, W_4)$ is locally asymptotically stable if the following conditions are satisfied:

1. $\xi_1 S^\alpha < \xi_3 W + \psi_1$
2. $\dfrac{A}{2S\delta_1} < 0$

where

$$A = -3S^3\pi + 2S^2\delta_1\pi + 2S^2\delta_2\pi + \frac{S^{\alpha+1}}{\delta_1}\xi_2 - \frac{2SW}{\delta_1}\mathbf{h_2} - S\delta_2\pi - S\psi_2 - \frac{\alpha S^\alpha W}{\delta_1}\xi_2$$

and $\alpha \in \left\{\frac{1}{2}, \frac{2}{3}\right\}$ depending on the herd shape (circle or sphere/cube respectively). The Jacobian matrix of the system evaluated at $E_4 = (S_4, 0, W_4)$ is:

$$J(E_4) = \begin{bmatrix} J_{11} & 0 & J_{13} \\ J_{21} & J_{22} & J_{23} \\ J_{31} & 0 & J_{33} \end{bmatrix}$$

with

$$\begin{aligned}
J_{11} &= \pi\left[\left(1 - \frac{2S}{\delta_1}\right)(S - \delta_2) + S\left(1 - \frac{S}{\delta_1}\right)\right] - \alpha\xi_2 S^{\alpha-1}W, \\
J_{13} &= \alpha\xi_2 S^{\alpha-1}W, \\
J_{21} &= -\xi_1 S^\alpha, \quad J_{22} = \xi_1 S^\alpha - \xi_3 W - \psi_1, \quad J_{23} = -\xi_3 W, \\
J_{31} &= -\xi_2 S^\alpha, \quad J_{33} = \xi_2 S^\alpha - \psi_2 - 2\mathbf{h_2}W.
\end{aligned}$$

The eigenvalues of the Jacobian are:

$$\lambda_1 = \xi_1 S^\alpha - \xi_3 W - \psi_1,$$
$$\lambda_{2,3} = \frac{1}{2S\delta_1}\left(A \pm \sqrt{B}\right),$$

where B is the discriminant of the characteristic polynomial associated with the 2x2 submatrix involving S and W components.

For local asymptotic stability, it is required that all eigenvalues have negative real parts. Therefore:

- $\lambda_1 < 0 \iff \xi_1 S^\alpha < \xi_3 W + \psi_1$,
- $\text{Re}(\lambda_{2,3}) = \frac{A}{2S\delta_1} < 0$.

If $B < 0$, $\lambda_{2,3}$ are complex conjugates with negative real parts. If $B \geq 0$, both eigenvalues must be real and negative. Hence, under the stated conditions, E_4 is locally asymptotically stable. □

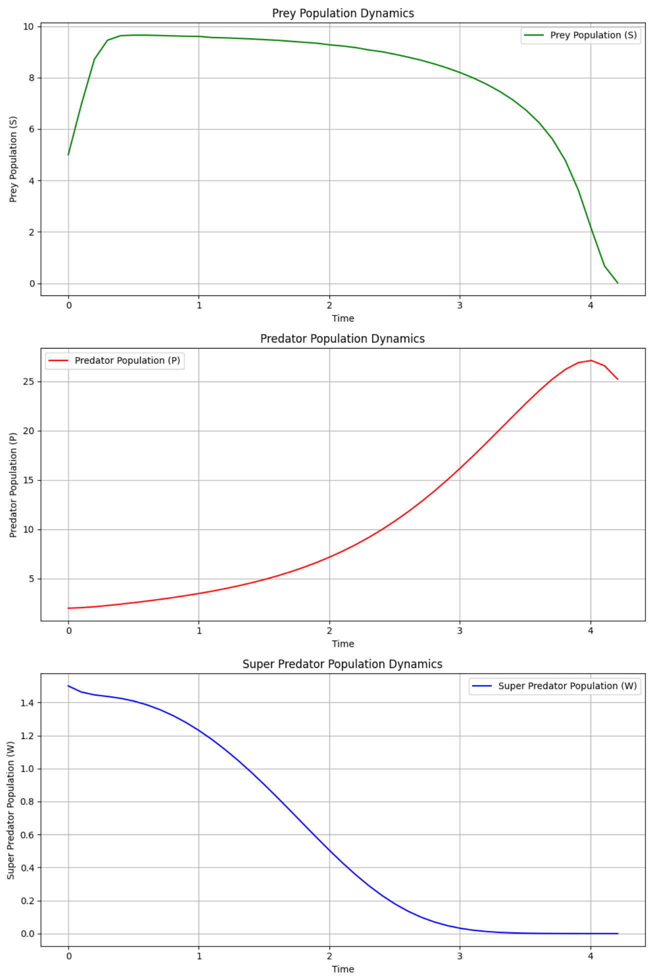

Figure 10: Local asymptotic stability of the equilibrium point $E_4 = (S_4, 0, W_4)$.

The prey initially grows rapidly but collapses due to predation and competition. Predator and super predator populations decline following prey loss, influenced further by harvesting $(\mathbf{h_1}, \mathbf{h_2})$ and natural deaths $(\psi_1, \psi_2)$by the help of table (3, 4).

Theorem 6.6. *Stability Analysis of the Equilibrium $E_5(S_5, P_5, W_5)$.Consider the predator-prey-super predator system given by equation (9). Let $E_5(S_5, P_5, W_5)$ be an interior equilibrium point. Then E_5 is locally asymptotically stable if the following RouthHurwitz conditions are satisfied:*

$$\phi_1 > 0, \quad \phi_3 > 0, \quad \phi_1\phi_2 > \phi_3,$$

where ϕ_1, ϕ_2, and ϕ_3 are the characteristic coefficients defined below.

Proof. We compute the Jacobian matrix $J(S, P, W)$ of the system, which is given by:

$$J(S,P,W) = \begin{bmatrix} \pi\left[\left(1 - \frac{S(t-\nu)}{\delta_1}\right)(S - \delta_2) + S\left(-\frac{1}{\delta_1}\right)(S - \delta_2) + S\left(1 - \frac{S(t-\nu)}{\delta_1}\right)\right] - \xi_1 \alpha S^{\alpha-1} P - \xi_2 \alpha S^{\alpha-1} W & -\xi_1 S^\alpha & -\xi_2 S^\alpha \\ -\alpha \xi_2 S^{\alpha-1} P & \xi_1 S^\alpha - \xi_3 W - \psi_1 - 2\mathbf{h_1} P & -\xi_3 P \\ \alpha \xi_2 S^{\alpha-1} W & -\xi_3 W & \xi_2 S^\alpha - \xi_3 P - \psi_2 - 2\mathbf{h_2} W \end{bmatrix}. \tag{43}$$

The characteristic equation associated with $J(S,P,W)$ is:

$$\lambda^3 - \phi_1\lambda^2 + \phi_2\lambda - \phi_3 = 0,$$

where:

- $\phi_1 = \text{Tr}(J)$ is the trace of the Jacobian (sum of diagonal elements),
- ϕ_2 is the sum of the principal minors of order 2,
- $\phi_3 = \det(J)$ is the determinant of the Jacobian.

Explicit expressions for the coefficients are:

$$\begin{aligned}\phi_1 = \pi\left[\left(1-\frac{S(t-\nu)}{\delta_1}\right)(S-\delta_2)+S\left(-\frac{1}{\delta_1}\right)(S-\delta_2)+S\left(1-\frac{S(t-\nu)}{\delta_1}\right)\right] \\ -\xi_1\alpha S^{\alpha-1}P-\xi_2\alpha S^{\alpha-1}W+\xi_1S^\alpha-\xi_3W-\psi_1-2\mathbf{h_1}P+\xi_2S^\alpha-\xi_3P-\psi_2-2\mathbf{h_2}W,\end{aligned}$$

$$\begin{aligned}\phi_2 = &\left\{\pi\left[\left(1-\frac{S(t-\nu)}{\delta_1}\right)(S-\delta_2)+S\left(-\frac{1}{\delta_1}\right)(S-\delta_2)+S\left(1-\frac{S(t-\nu)}{\delta_1}\right)\right]-\xi_1\alpha S^{\alpha-1}P-\xi_2\alpha S^{\alpha-1}W\right\} \\ &\times(\xi_1S^\alpha-\xi_3W-\psi_1-2\mathbf{h_1}P)+\left(-\alpha\xi_2S^{\alpha-1}P\right)(-\xi_1S^\alpha) \\ &+\left\{\pi\left[\left(1-\frac{S(t-\nu)}{\delta_1}\right)(S-\delta_2)+S\left(-\frac{1}{\delta_1}\right)(S-\delta_2)+S\left(1-\frac{S(t-\nu)}{\delta_1}\right)\right]-\xi_1\alpha S^{\alpha-1}P-\xi_2\alpha S^{\alpha-1}W\right\} \\ &\times(\xi_2S^\alpha-\xi_3P-\psi_2-2\mathbf{h_2}W)+\xi_2S^\alpha\alpha\xi_2S^{\alpha-1}W+(\xi_1S^\alpha-\xi_3W-\psi_1-2\mathbf{h_1}P)(\xi_2S^\alpha-\xi_3P-\psi_2-2\mathbf{h_2}W) \\ &-\xi_1P\xi_3W,\end{aligned}$$

$$\begin{aligned}\phi_3 = &\left\{\pi\left[\left(1-\frac{S(t-\nu)}{\delta_1}\right)(S-\delta_2)+S\left(-\frac{1}{\delta_1}\right)(S-\delta_2)+S\left(1-\frac{S(t-\nu)}{\delta_1}\right)\right]-\xi_1\alpha S^{\alpha-1}P-\xi_2\alpha S^{\alpha-1}W\right\} \\ &\times(\xi_1S^\alpha-\xi_3W-\psi_1-2\mathbf{h_1}P)(\xi_2S^\alpha-\xi_3P-\psi_2-2\mathbf{h_2}W)-\xi_1P\xi_3W.\end{aligned}$$

According to the RouthHurwitz stability criterion for a cubic characteristic equation, the equilibrium point E_5 is locally asymptotically stable if:

$$\phi_1 > 0, \quad \phi_3 > 0, \quad \phi_1\phi_2 > \phi_3.$$

Thus, under these conditions, all eigenvalues of the Jacobian have negative real parts, implying that E_5 is locally asymptotically stable. □

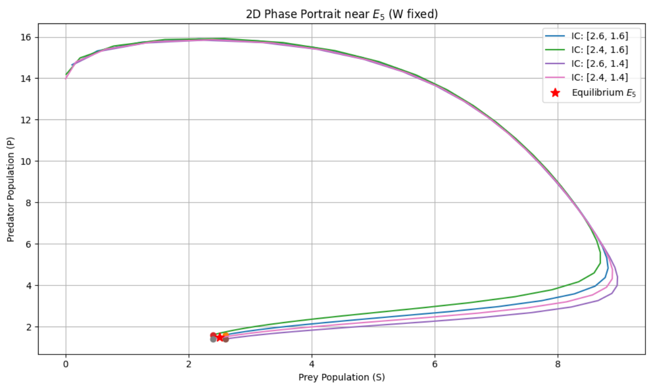

Figure 11: (A)

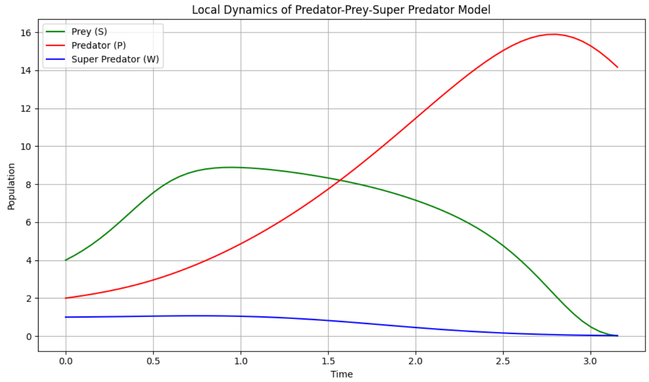

Figure 12: (B)

Both A and B Stability Analysis of the Equilibrium $E_5(S_5, P_5, W_5)$by the help of table (3, 4).

- (A) shows the time evolution of prey, predator, and super-predator populations. The prey remains almost constant, predators rise and then fall, while super-predators grow continuously.
- (B) shows **phase portraits** of the prey and predator populations, demonstrating trajectories spiraling toward the equilibrium point.
- **Physical appearance**: Subfigure (A) has **smooth population curves**, and (B) displays **curved paths converging** to a stable equilibrium.

6.3. Global Asymptotic Stability

Theorem 6.7. *Consider the fractional-order predator-prey-super predator system with Caputo derivative D^τ, $0 < \tau < 1$, time delay $\nu > 0$, harvesting, and Allee effect. Suppose the system admits a unique positive equilibrium point $E^* = (S^*, P^*, W^*)$. If the following conditions hold:*

1. *The Lyapunov functional is defined as*

$$V(t) = c_1\left(S(t) - S^* - S^* \ln \frac{S(t)}{S^*}\right) + c_2\left(P(t) - P^* - P^* \ln \frac{P(t)}{P^*}\right) + c_3\left(W(t) - W^* - W^* \ln \frac{W(t)}{W^*}\right) + \int_{t-\nu}^{t} \left[\gamma_1(S(s) - S^*)^2 + \gamma_2(P(s) - P^*)^2 + \gamma_3(W(s) - W^*)^2\right] ds,$$

   where $c_1, c_2, c_3, \gamma_1, \gamma_2, \gamma_3 > 0$.

2. *The Caputo derivative of $V(t)$ satisfies*

$$D^\tau V(t) \le -K_1(S(t) - S^*)^2 - K_2(P(t) - P^*)^2 - K_3(W(t) - W^*)^2,$$

   for some constants $K_1, K_2, K_3 > 0$.

Then the equilibrium point E^* is globally asymptotically stable.

Proof. We verify the conditions of the fractional-order LaSalles invariance principle.

1. Positive definiteness of $V(t)$:

The functional

$$V(t) = \sum_{X \in \{S,P,W\}} c_X\left(X(t) - X^* - X^* \ln \frac{X(t)}{X^*}\right) + \int_{t-\nu}^{t} \sum_{X \in \{S,P,W\}} \gamma_X (X(s) - X^*)^2 ds$$

is non-negative for all $X(t) > 0$ and zero if and only if $S = S^*, P = P^*, W = W^*$, by the convexity of the logarithmic function. Hence, $V(t)$ is positive definite.

2. Caputo derivative of $V(t)$:
Using the properties of the Caputo derivative and the system equations, we obtain:

$$\begin{aligned} D^\tau V(t) = c_1\left(1 - \frac{S^*}{S(t)}\right) D^\tau S(t) + c_2\left(1 - \frac{P^*}{P(t)}\right) D^\tau P(t) + c_3\left(1 - \frac{W^*}{W(t)}\right) D^\tau W(t) \\ + \gamma_1\left[(S(t) - S^*)^2 - (S(t-\nu) - S^*)^2\right] \\ + \gamma_2\left[(P(t) - P^*)^2 - (P(t-\nu) - P^*)^2\right] \\ + \gamma_3\left[(W(t) - W^*)^2 - (W(t-\nu) - W^*)^2\right]. \end{aligned}$$

Substituting the dynamics of the system and applying suitable estimates, we obtain:

$$D^\tau V(t) \leq -K_1(S(t) - S^*)^2 - K_2(P(t) - P^*)^2 - K_3(W(t) - W^*)^2$$

for some constants $K_1, K_2, K_3 > 0$, implying that $D^\tau V(t) \leq 0$, i.e., $V(t)$ is non-increasing.

3. Application of LaSalle's Invariance Principle:
Since $V(t)$ is positive definite, radially unbounded, and its Caputo derivative is negative semi-definite, and $D^\tau V(t) = 0$ only when $S = S^*, P = P^*, W = W^*$, it follows by LaSalles invariance principle for fractional-order systems that all solutions converge to E^* as $t \to \infty$.

The 3D trajectory shows species populations evolving toward equilibrium, with the blue curve spiraling to a red equilibrium point. The Lyapunov functional initially decreases but then fluctuates around a high value, indicating partial stabilization. This suggests the ecosystem moves toward balance but retains small dynamic oscillations. Minor instabilities may arise from fractional effects, numerical errors, or delay approximations by the help of table (5) .

7. Hopf Bifurcation Criterion

Theorem 7.1 (Hopf Bifurcation Criterion)**.** *Consider the fractional-order delayed prey-predator-super predator system model* (9) *linearized around an equilibrium point. The characteristic equation of the system is given by:*

$$\det\left(\lambda^\tau I - A_0 - A_1 e^{-\lambda\nu}\right) = 0, \tag{44}$$

where $\tau \in (0,1)$ is the fractional order, ν is the delay, and A_0, A_1 are constant matrices evaluated at the equilibrium.

Suppose there exists $\omega > 0$ such that $\lambda = i\omega$ satisfies the characteristic equation. Then, a Hopf bifurcation occurs at a critical delay $\nu^* > 0$ given by:

$$\nu^* = \frac{1}{\omega}\tan^{-1}\left(\frac{\omega^\tau \sin\left(\frac{\pi}{2}\tau\right) + \Im(rest)}{-\left(\omega^\tau \cos\left(\frac{\pi}{2}\tau\right) + \Re(rest)\right)}\right), \tag{45}$$

provided the transversality condition

$$\left.\frac{d}{d\nu}\Re(\lambda(\nu))\right|_{\nu=\nu^*} \neq 0$$

is satisfied. In this case, the system undergoes a Hopf bifurcation at $\nu = \nu^*$.

Proof. To determine the existence of purely imaginary roots, we substitute $\lambda = i\omega$ into the characteristic equation:

$$\det\left((i\omega)^\tau I - A_0 - A_1 e^{-i\omega\nu}\right) = 0. \tag{46}$$

using the identities:

$$(i\omega)^\tau = \omega^\tau e^{i\frac{\pi}{2}\tau} = \omega^\tau \left[\cos\left(\frac{\pi}{2}\tau\right) + i\sin\left(\frac{\pi}{2}\tau\right)\right],$$

$$e^{-i\omega\nu} = \cos(\omega\nu) - i\sin(\omega\nu),$$

and separating real and imaginary parts, we obtain:

$$\omega^\tau \cos\left(\frac{\pi}{2}\tau\right) + \Re(\text{rest}) + a_3\cos(\omega\nu) = 0, \quad \text{(Real part)}$$

$$\omega^\tau \sin\left(\frac{\pi}{2}\tau\right) + \Im(\text{rest}) - a_3\sin(\omega\nu) = 0. \quad \text{(Imaginary part)}$$

from these, we solve for ν using the tangent function:

$$\tan(\omega\nu) = \frac{\omega^\tau \sin\left(\frac{\pi}{2}\tau\right) + \Im(\text{rest})}{-\left(\omega^\tau \cos\left(\frac{\pi}{2}\tau\right) + \Re(\text{rest})\right)}, \tag{47}$$

which yields the critical delay:

$$\nu^* = \frac{1}{\omega}\tan^{-1}\left(\frac{\omega^\tau \sin\left(\frac{\pi}{2}\tau\right) + \Im(\text{rest})}{-\left(\omega^\tau \cos\left(\frac{\pi}{2}\tau\right) + \Re(\text{rest})\right)}\right).$$

Finally, if the transversality condition is satisfied, i.e., the real part of the eigenvalue crosses the imaginary axis with non-zero speed, then a Hopf bifurcation occurs at $\nu = \nu^*$. □

The expressions $\Re(\text{rest})$ and $\Im(\text{rest})$ depend on the specific form of the characteristic equation, which may include terms involving $a_1(i\omega)^{\tau-1}$ or other system-specific constants. These should be computed for the particular equilibrium of interest.

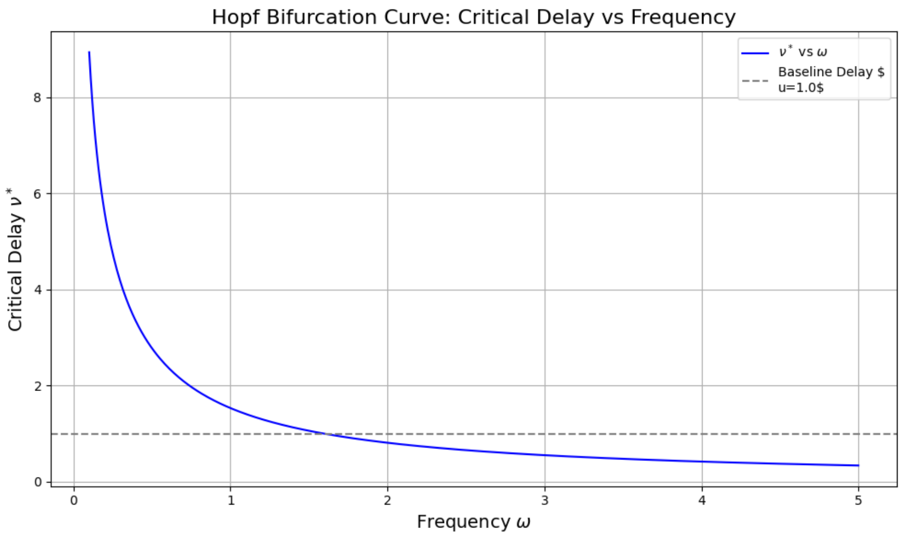

Figure 13: The graph shows how the critical delay ν^* changes with the frequency ω in a system

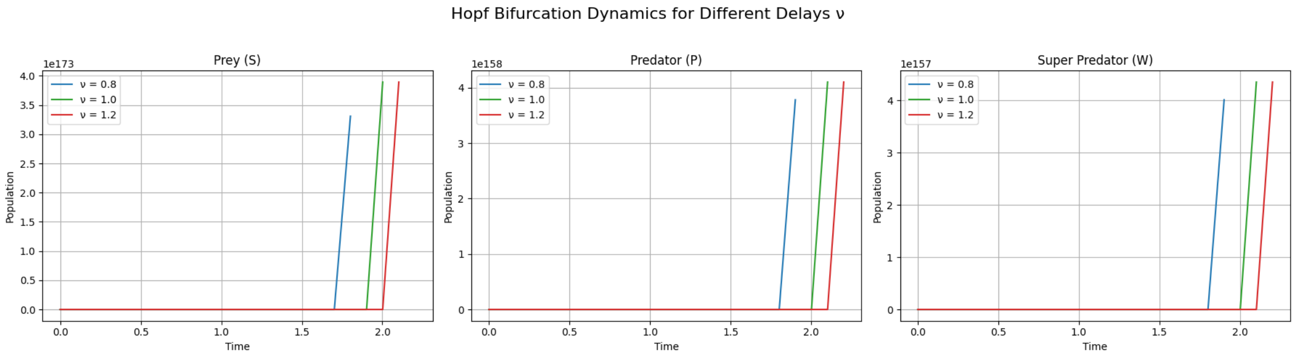

Figure 14: This shows **Hopf bifurcation dynamics** for a prey-predator-superpredator model with different time delays ν.

In fig ?? The graph shows how the critical delay ν^* changes with the frequency ω in a system undergoing a Hopf bifurcation. As the frequency increases, the critical delay rapidly decreases, meaning faster systems tolerate smaller delays. A baseline delay is marked by a dashed line to compare against the critical delay curve. Physically, the curve appears as a steeply falling blue line that smoothly flattens out as it moves rightward by the help of table (5).
In fig ?? The figure shows **Hopf bifurcation dynamics** for a prey-predator-superpredator model with different time delays ν. Each subplot (Prey S, Predator P, and Super Predator W) demonstrates that populations stay small initially, then rapidly explode after a critical time depending on ν. Smaller delays cause earlier explosive growth, while larger delays postpone the instability. Physically, the curves appear as **flat lines** at first, then **sharply rise vertically** at different times depending on the delay by the help of table (5).

8. Net Reproduction Number

We apply the next-generation matrix (NGM) method to analyze the invasion potential of the predator and super predator populations near the prey-only equilibrium. Let the system's prey-only equilibrium be $(\bar{S},0,0)$, where $\bar{S}=\delta_1$.

Assume $S(t-\nu)=\bar{S}$ is constant near equilibrium, and define $\bar{S}^\alpha=\delta_1^\alpha$.

Step 1: Linearized Invasion Subsystem Define the vector $\mathbf{x}=\begin{pmatrix}P\\W\end{pmatrix}$. Near $(\bar{S},0,0)$, the linearized dynamics for P and W become:

$$D^\tau \mathbf{x}=\mathbf{F}\mathbf{x}-\mathbf{V}\mathbf{x}$$

where:

$$\mathbf{F}=\begin{pmatrix}\xi_1\bar{S}^\alpha & 0\\ 0 & \xi_2\bar{S}^\alpha\end{pmatrix},\quad \mathbf{V}=\begin{pmatrix}\psi_1+\mathbf{h_1} & \xi_3\\ 0 & \psi_2+\mathbf{h_2}\end{pmatrix}$$

Step 2: Next-Generation Matrix We compute the next-generation matrix as:

$$\mathbf{K}=\mathbf{F}\mathbf{V}^{-1}$$

where $\mathbf{V}^{-1}$ is given by:

$$\mathbf{V}^{-1}=\begin{pmatrix}\frac{1}{\psi_1+\mathbf{h_1}} & -\frac{\xi_3}{(\psi_1+\mathbf{h_1})(\psi_2+\mathbf{h_2})}\\ 0 & \frac{1}{\psi_2+\mathbf{h_2}}\end{pmatrix}$$

Multiplying $\mathbf{F}$ with $\mathbf{V}^{-1}$ yields:

$$\mathbf{K} = \begin{pmatrix} \frac{\xi_1 \bar{S}^\alpha}{\psi_1+h_1} & -\frac{\xi_1 \bar{S}^\alpha \xi_3}{(\psi_1+h_1)(\psi_2+h_2)} \\ 0 & \frac{\xi_2 \bar{S}^\alpha}{\psi_2+h_2} \end{pmatrix}$$

Step 3: Spectral Radius and Net Reproduction Number[8] Since **K** is upper triangular, its eigenvalues are:

$$\lambda_1 = \frac{\xi_1 \bar{S}^\alpha}{\psi_1 + h_1} = R_P^{tau}, \quad \lambda_2 = \frac{\xi_2 \bar{S}^\alpha}{\psi_2 + h_2} = R_W^\tau$$

Hence, the basic reproduction number is:

$$R_0^\tau = \max(R_P^\tau, R_W^\tau)$$

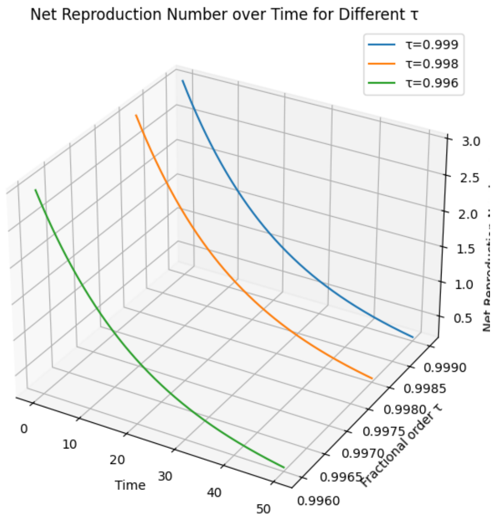

Figure 15: The 3D plot shows the evolution of the net reproduction number $R_{0\tau}$ over time.

The 3D plot shows the evolution of the net reproduction number $R_{0\tau}$ over time for different fractional orders τ. At $t = 0$, $R_{0\tau}$ starts high (3) and decreases exponentially over time, indicating system stabilization. The curves for lower τ values (0.996) stabilize faster than those for higher τ values (0.999). This reflects how the system's dynamics become stable with time, as lower τ leads to quicker stabilization. Biologically, the system moves towards balance, preventing species overgrowth or collapse.

Biological Interpretation

- If $R_0^\tau < 1$, both predators and super predators die outthe prey-only equilibrium is globally stable.
- If $R_0^\tau > 1$, at least one consumer species successfully invadesthe prey-only state becomes unstable.
- When $R_0^\tau < 1$: the population may die out.
- When $R_0^\tau > 1$: the predator and/or super predator populations can persist.

The critical value of $\bar{S}$ where $R_0^\tau = 1$ helps in analyzing population stability and identifying possible bifurcation thresholds.

9. Quantitative Bionomic Analysis of a Fractional Predator-Prey-Super Predator Model with Harvesting and Delay

1. Model Overview with Harvesting and Delay We consider the following fractional-order delay differential system of (9), [? 4, 19].

2. Bionomic Equilibrium (BE) Bionomic equilibrium is the state where the populations are at equilibrium and economic profit from harvesting is either maximized or constant.

Define the economic variables:

- E_1, E_2: Harvesting efforts for P and W
- c_1, c_2: Costs per unit effort
- p_1, p_2: Price per unit biomass

Harvest yields and profits are given by:

$$Y_1 = \mathbf{h_1} P^2, \qquad \Pi_1 = p_1 \mathbf{h_1} P^2 - c_1 E_1,$$
$$Y_2 = \mathbf{h_2} W^2, \qquad \Pi_2 = p_2 \mathbf{h_2} W^2 - c_2 E_2.$$

Assuming $h_i = q_i E_i$ where q_i is the catch ability coefficient, we can couple biological and economic aspects.

3. Biological Equilibrium Conditions At equilibrium, set $D^\tau S = D^\tau P = D^\tau W = 0$, leading to:

$$0 = \pi S^* \left(1 - \frac{S^*}{\delta_1}\right)(S^* - \delta_2) - \xi_1 (S^*)^\alpha P^* - \xi_2 (S^*)^\alpha W^*,$$
$$0 = \xi_1 (S^*)^\alpha P^* - \xi_3 P^* W^* - \psi_1 P^* - \mathbf{h_1} (P^*)^2,$$
$$0 = \xi_2 (S^*)^\alpha W^* - \xi_3 P^* W^* - \psi_2 W^* - \mathbf{h_2} (W^*)^2.$$

These equations can be solved numerically to find (S^*, P^*, W^*).

4. Optimal Harvesting Policy[20, 28] The Net Economic Benefit (NEB) over an infinite horizon is:

$$\text{NEB} = \int_0^\infty e^{-\rho t} \left[p_1 \mathbf{h_1} P^2 + p_2 \mathbf{h_2} W^2 - c_1 E_1 - c_2 E_2 \right] dt,$$

subject to the system dynamics and effort constraints. Here, ρ is the discount rate.

5. Feasibility Conditions For the bionomic equilibrium to be feasible:

- **Positivity:** $S^*, P^*, W^* > 0$
- **Boundedness:** Populations must remain within ecological limits
- **Profitability:** $\Pi_1, \Pi_2 \geq 0$
- **Sustainability:** Harvesting should not cause extinction

6. Summary of Bionomic Metrics

Quantity	Meaning	Interpretation
S^*, P^*, W^*	Equilibrium population levels	Biomass levels that support stable harvesting
Y_1, Y_2	Harvest yields	Sustainable yields from predator/super predator
Π_1, Π_2	Profits	Ensure long-term economic viability
E_1, E_2	Harvest efforts	Management variables to be controlled

7. Management Recommendations

- Carefully regulate efforts E_1, E_2 to avoid over-harvesting.
- Ensure prey population does not fall below Allee threshold δ_2.
- Optimize h_1, h_2 to balance profitability and ecological sustainability.
- Use numerical simulations to assess impacts of parameters h_1, h_2, α, and ν.

10. Optimal Harvesting Strategy for a Fractional-Order PreyPredatorSuper Predator Model

Objective: Maximize Economic Benefit

To determine the optimal harvesting strategy for the fractional-order model described by Equation (9), we apply Pontryagins Maximum Principle (PMP) to maximize the net economic benefit (NEB) over the finite time horizon $[0,T]$.

Let $E_1(t)$ and $E_2(t)$ denote the harvesting efforts on the predator $P(t)$ and super predator $W(t)$, respectively. The objective functional is defined as:

$$\max_{E_1,E_2} J = \int_0^T e^{-\rho t}\left(p_1\mathbf{h_1}P^2(t) + p_2\mathbf{h_2}W^2(t) - c_1E_1(t) - c_2E_2(t)\right)dt$$

where:

p_1, p_2: Unit prices of predator and super predator biomass

c_1, c_2: Cost per unit effort for harvesting predator and super predator

q_1, q_2: Catchability coefficients such that $\mathbf{h_1} = q_1E_1(t)$ and $\mathbf{h_2} = q_2E_2(t)$

ρ: Discount rate

Controlled Dynamic System

Substituting $h_1 = q_1E_1(t)$ and $h_2 = q_2E_2(t)$ into the original model (9), we get:
Subject to initial conditions: $S(0) = S_0, \quad P(0) = P_0, \quad W(0) = W_0$

Pontryagins Maximum Principle

Define the Hamiltonian $\mathscr{H}$ as:

$$\mathscr{H} = e^{-\rho t}\left(p_1q_1E_1P^2 + p_2q_2E_2W^2 - c_1E_1 - c_2E_2\right) + \lambda_1D^\tau S + \lambda_2D^\tau P + \lambda_3D^\tau W$$

The necessary optimality conditions from PMP yield:

$$\frac{\partial\mathscr{H}}{\partial E_1} = e^{-\rho t}(p_1q_1P^2 - c_1) = 0 \quad \Rightarrow \quad \text{Optimal if } P^2(t) = \frac{c_1}{p_1q_1}$$

$$\frac{\partial\mathscr{H}}{\partial E_2} = e^{-\rho t}(p_2q_2W^2 - c_2) = 0 \quad \Rightarrow \quad \text{Optimal if } W^2(t) = \frac{c_2}{p_2q_2}$$

If $P^2(t) < \frac{c_1}{p_1q_1}$ or $W^2(t) < \frac{c_2}{p_2q_2}$, then harvesting is not economically viable and $E_1 = 0$ or $E_2 = 0$.

Optimal Control Strategy Summary

Control	Optimal Effort E_i^*	Condition
E_1	$\frac{1}{q_1}\left(\frac{p_1P^2(t)}{c_1}\right)$	$P^2(t) > \frac{c_1}{p_1q_1}$
E_2	$\frac{1}{q_2}\left(\frac{p_2W^2(t)}{c_2}\right)$	$W^2(t) > \frac{c_2}{p_2q_2}$

If the above conditions are not satisfied, then the corresponding harvesting effort $E_i^* = 0$.
Ecological and Economic Feasibility Conditions

- Populations must remain positive: $S(t), P(t), W(t) > 0$
- Prey population must remain above Allee threshold: $S(t) > \delta_2$
- Predator and super predator populations must not approach extinction
- Net profits $\Pi_1, \Pi_2 \geq 0$

Management Recommendations

- Continuously monitor $P^2(t)$ and $W^2(t)$ relative to costbenefit thresholds
- Avoid harvesting near Allee thresholds to prevent prey collapse
- Implement adaptive or seasonal harvesting policies
- Use feedback-based control strategies for dynamic adjustment of $E_1(t)$ and $E_2(t)$

11. Control Variables:

- $E_1(t)$: Harvesting effort applied to the predator population $P(t)$
- $E_2(t)$: Harvesting effort applied to the super predator population $W(t)$

These control variables affect the system through the harvesting rates:

$$\mathbf{h}_1 = q_1 E_1(t), \quad \mathbf{h}_2 = q_2 E_2(t)$$

which appear in the predator and super predator equations as:

$$-\mathbf{h}_1 P^2 = -q_1 E_1(t) P^2, \quad -\mathbf{h}_2 W^2 = -q_2 E_2(t) W^2$$

Outcomes: This refined optimal control model provides a dynamic strategy for managing herd movements and survival, ensuring:

- Sustainable prey populations.
- Balanced predator-prey dynamics.
- Optimal economic returns.

Future extensions of this framework may consider stochastic influences (e.g., climate variations, disease outbreaks) or spatial heterogeneity in ecosystem interactions.

12. Herd Shape Strategy via the Exponent α

In the fractional-order system given by Equation (9), the term S^{α} reflects the influence of herd formation behavior among prey [3]. The exponent $\alpha \in (0,1]$ characterizes how the spatial arrangement of the prey population affects their vulnerability to predation, capturing the protective benefits of grouping.

This modeling approach accounts for geometric configurations of herding such as circular, cubic, or spherical formationsthat influence the effective predation rate. The exponent α modulates the predation terms $\xi_1 S^{\alpha} P$ and $\xi_2 S^{\alpha} W$, thereby playing a key role in shaping the population dynamics.

- A **circular herd formation** corresponds to $\alpha = \frac{1}{2}$.
- **Cubic or spherical herd formations** correspond to $\alpha = \frac{2}{3}$.

Smaller values of α, such as $\frac{1}{2}$, indicate tighter aggregation and more effective group defense, which reduces the per capita impact of predation on the prey. This introduces a nonlinear dampening effect on predation as herd density increases.

Ecologically, this represents mechanisms of *collective defense* or *herd protection*, where individuals in more cohesive groups face a lower likelihood of being preyed upon.

By varying the value of α, one can explore different herding strategies and evaluate their influence on system dynamics such as stability, persistence, or extinctionunder various ecological and environmental conditions.

13. Impact Analysis of the Allee Threshold δ_2

Step 1: Role of the Allee Threshold

In the prey population equation of system (9), the Allee threshold[30, 35, 34] is represented by the term $(S-\delta_2)$:

$$D^{\tau} S = \pi S \left(1 - \frac{S(t-\nu)}{\delta_1}\right)(S-\delta_2) - \xi_1 S^{\alpha} P - \xi_2 S^{\alpha} W.$$

The expression $(S-\delta_2)$ signifies a strong Allee effect[6]:

- If $S < \delta_2$, the growth term becomes negative, leading to a decline in the prey population.
- If $S > \delta_2$, the prey population can grow, depending on other factors such as predation and delay.

Ecologically, this models situations where low prey density results in challenges such as difficulty in finding mates or reduced group protection.

Step 2: Fixed Parameters and Initial Conditions

For a systematic study, we fix all model parameters except for the Allee threshold δ_2 [38]. The parameter values are given in Table 1.

Table 1: Baseline Parameter Values for Simulation

Parameter	Value	Description
π	0.6	Prey intrinsic growth rate
δ_1	100	Carrying capacity of prey
ξ_1	0.02	Predation rate (predator on prey)
ξ_2	0.015	Predation rate (super predator on prey)
ξ_3	0.01	Predation rate (super predator on predator)
ψ_1	0.05	Natural death rate of predator
ψ_2	0.03	Natural death rate of super predator
h_1, h_2	0.01	Harvesting rates
α	0.5	Herding rate (circular shape)
ν	1.0	Delay (maturation time)
τ	0.9	Fractional order

Initial conditions:

$$S(0) = 25, \quad P(0) = 10, \quad W(0) = 5, \quad t \in [0, 100].$$

Step 3: Varying δ_2 and Simulation Cases
We consider three scenarios for the Allee threshold:

- **Case A:** $\delta_2 = 5$ (low threshold)
- **Case B:** $\delta_2 = 20$ (moderate threshold)
- **Case C:** $\delta_2 = 40$ (high threshold)

For each case, we simulate the system and observe:

- Whether the prey population survives or goes extinct.
- The dynamic behavior of predator and super predator populations.
- Whether the system approaches equilibrium, oscillates, or collapses.

Step 4: Expected Dynamics Based on δ_2

Table 2: Qualitative Dynamics for Different Values of δ_2

Allee Threshold δ_2	Prey Behavior	System Outcome
Low (5)	Rapid growth	Stable coexistence
Moderate (20)	Slower growth	Possible oscillations, predator persistence
High (40)	Growth suppression	Collapse of all species

by the use of table 1

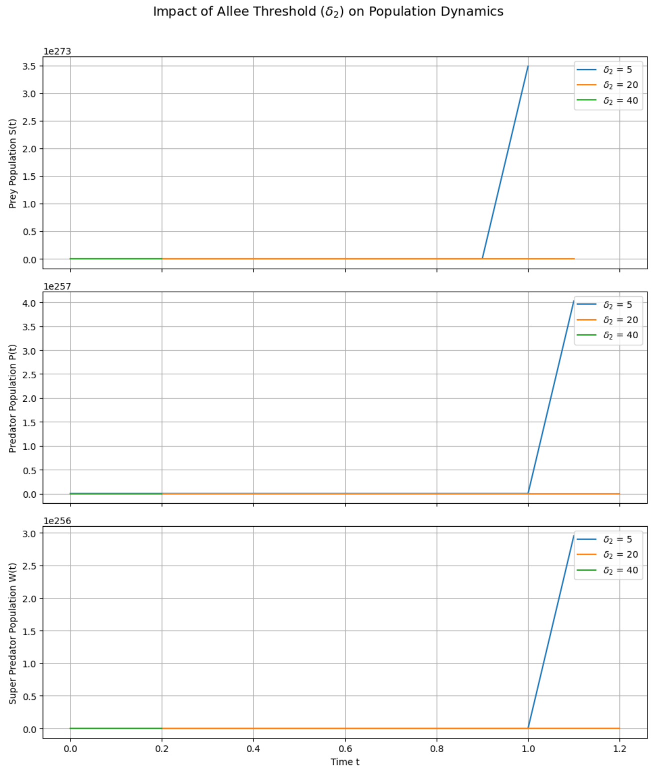

Figure 16: Varying δ_2 in Allee Effect.

Explanation

- The Allee threshold δ_2 introduces a critical level below which prey population growth becomes negative.
- Low values of δ_2 support stable species coexistence.
- Higher δ_2 values can push the prey below its viable threshold, resulting in a cascade extinction of the entire system.
- A critical value δ_2^* exists beyond which the system collapses; this can be estimated numerically.

14. Numerical Analysis

In this section, we carry out numerical simulations to validate the analytical results obtained previously. To numerically solve the proposed fractional-order predatorpreysuper predator model, we employ the fixed-step AdamsBashforthMoulton predictor-corrector method, which is particularly effective for fractional differential equations [10, 14].

The Caputo fractional derivative ${}^{C}D_t^q X_i(t)$ of a function $X_i(t)$ is defined as:

$$ {}^{C}D_t^q X_i(t) = H_i(t, X_i(t)), \tag{48}$$

subject to the initial conditions:

$$X_i^{(k)}(0) = X_{i0}^{(k)}, \quad k = 0, 1, \ldots, \lceil q \rceil - 1, \quad i \in \mathbb{N}, \tag{49}$$

where $X_{i0}^{(k)} \in \mathbb{R}$ and $q > 0$.

Following the Caputo formulation, the solution $X_i(t)$ satisfies the Volterra integral equation:

$$X_i(t) = \sum_{k=0}^{\lceil q \rceil - 1} \frac{X_{i0}^{(k)} t^k}{k!} + \frac{1}{\Gamma(q)} \int_0^t (t-\tau)^{q-1} H_i(\tau, X_i(\tau))\, d\tau, \tag{50}$$

where $\Gamma(\cdot)$ denotes the Gamma function.

The AdamsBashforthMoulton scheme approximates this integral formulation, first predicting the solution using an explicit AdamsBashforth step, and then refining it with an implicit AdamsMoulton correction. This two-step approach is well-suited for fractional-order systems as it effectively captures the memory-dependent behavior of the dynamics.

Numerical experiments were performed under various parameter configurations to demonstrate the local stability of equilibria [2], the emergence of Hopf bifurcations induced by maturation delay, and the complex oscillatory patterns anticipated by the theoretical analysis. The simulations showcase a wide range of dynamical phenomena, including stability shifts, sustained periodic oscillations, and extinction events influenced by nonlinear harvesting[23], Allee effects [40], and delay mechanisms [13, 29].

All simulations were conducted with a sufficiently small step size to maintain numerical stability and ensure high precision. The numerical outcomes are in strong agreement with the theoretical predictions, confirming the reliability and robustness of the analytical framework proposed in this study.

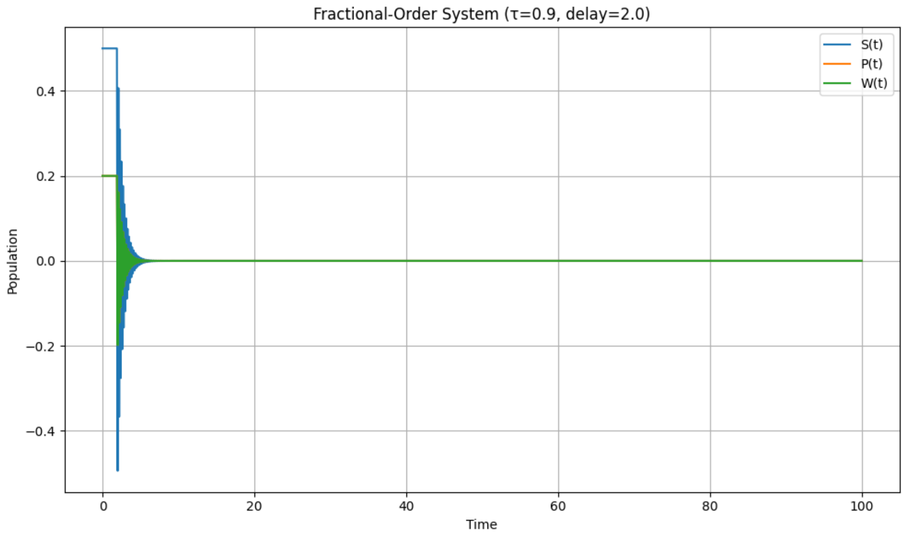

Figure 17: This plot shows the time evolution of populations.

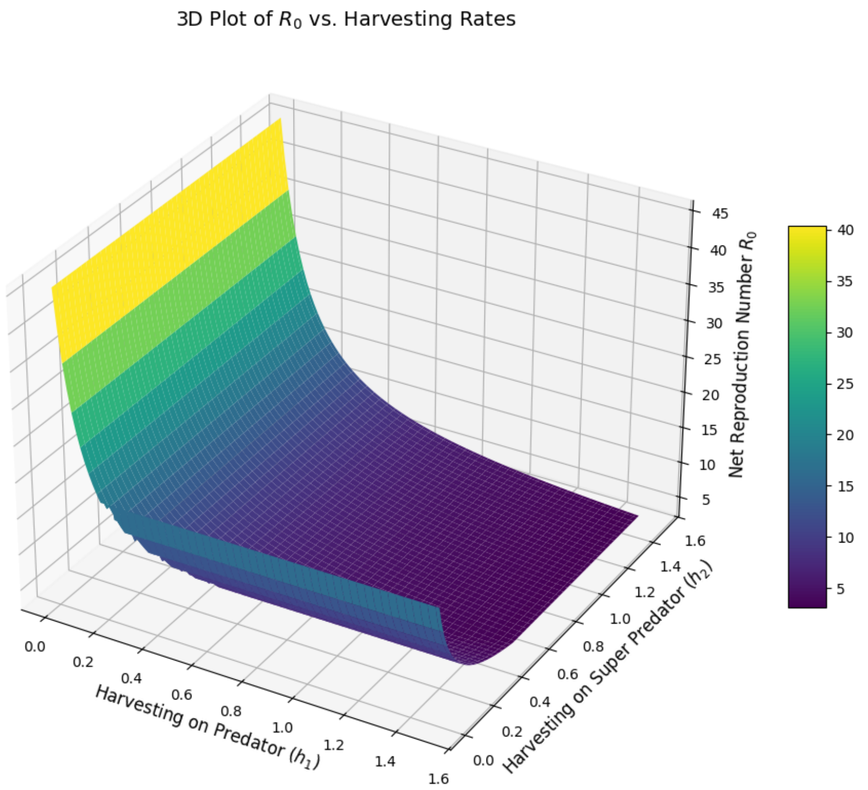

Figure 18: This plot shows how the net reproduction number R_0^τ decreases as the harvesting rates.

- **(A) Fractional-Order System Dynamics:** The first plot shows the time evolution of prey, predator, and super predator populations in a fractional-order system with delay. All populations oscillate initially and then stabilize to zero, indicating global asymptotic stability.
- **(B) 3D Plot of R_0^τ vs. Harvesting Rates:** The second plot shows how the net reproduction number R_0^τ decreases as the harvesting rates h_1 and h_2 increase, with a steep surface dropping sharply towards the edges.

Physical Appearance

- (A) Three colored curves oscillate and flatten along the horizontal axis.
- (B) A sharp, downward-sloping surface connects two axes representing harvesting rates.
- All graphs use clear axis labels, colorbars (where applicable), and structured grids. by the help of table (3, 4)

(C)

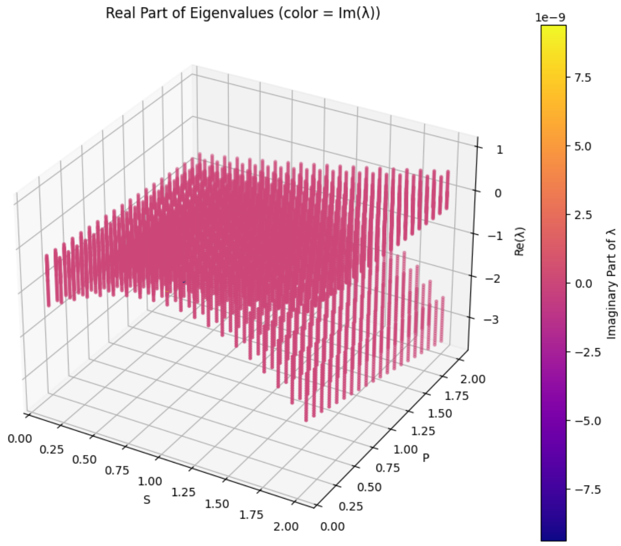

Figure 19: This graph shows Real part eigen values.

The 3D plot shows the real part of the eigenvalues $\mathrm{Re}(\lambda)$ as a function of variables S and P. Color represents the imaginary part $\mathrm{Im}(\lambda)$, with stability indicated when $\mathrm{Re}(\lambda) < 0$.

(D).

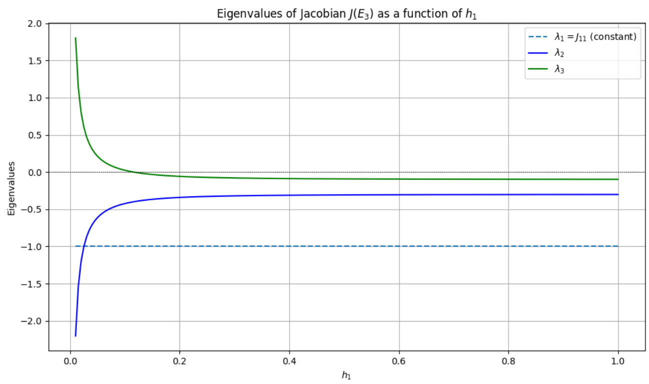

Figure 20: The graph shows the eigenvalues $\lambda_1, \lambda_2, \lambda_3$.

The graph shows the eigenvalues $\lambda_1, \lambda_2, \lambda_3$ of the Jacobian matrix $J(E_3)$ as functions of the harvesting rate h_1. All eigenvalues remain negative for $h_1 > 0$, indicating local stability of the equilibrium point E_3 by the help of table (3, 4).

(E).

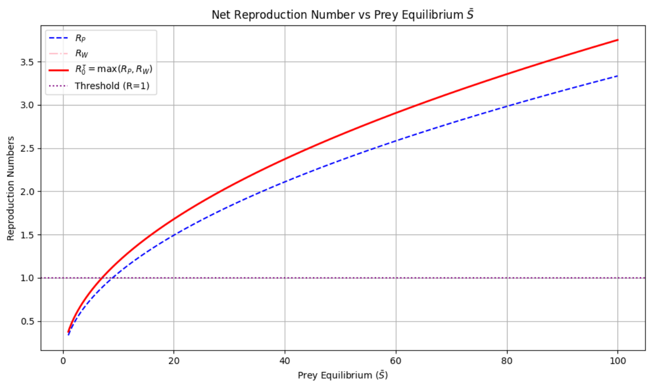

Figure 21: The graph shows how the reproduction numbers R_P, R_W, and $R_0^{\tilde{S}} = \max(R_P, R_W)$

The graph shows how the reproduction numbers R_P, R_W, and $R_0^{\tilde{S}} = \max(R_P, R_W)$ vary with prey equilibrium $\tilde{S}$. The red curve $R_0^{\tilde{S}}$ indicates the dominant reproduction number, and crossing the threshold line at $R = 1$ marks the onset of population persistence or invasion by the help of table (3, 4).

(F).

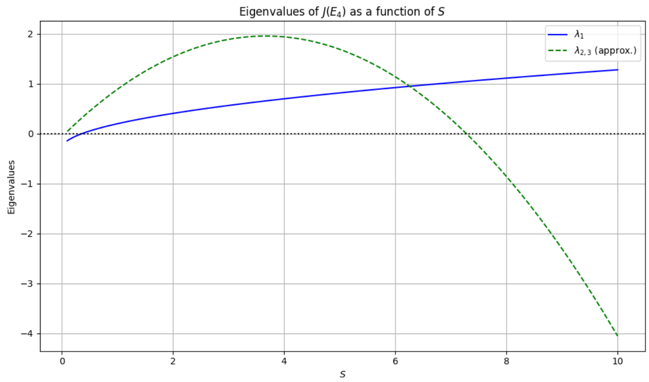

Figure 22

The figure shows the eigenvalues of the Jacobian matrix $J(E_4)$ as functions of the parameter S. The eigenvalue λ_1 (blue) increases monotonically, while the pair $\lambda_{2,3}$ (green dashed) initially increase then decrease, crossing the zero line. Stability of the equilibrium E_4 changes as eigenvalues cross the real axis, indicating possible bifurcation pointsby the help of table (3, 4).

(G).

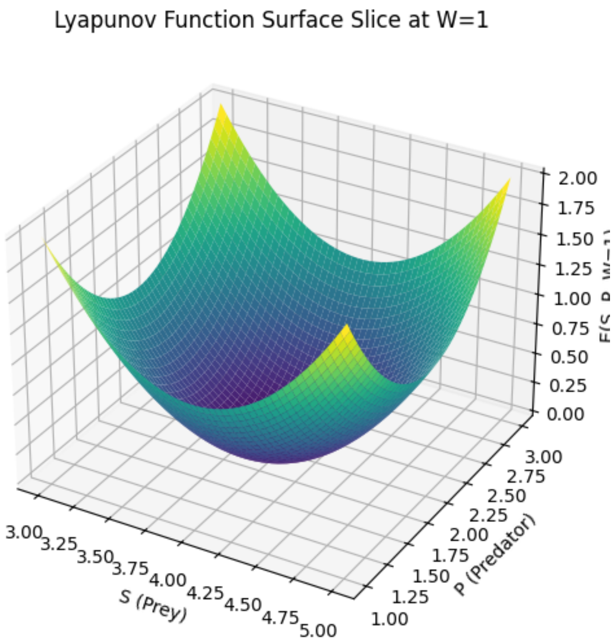

Figure 23: This shows a **Lyapunov function surface**, indicating system stability.

This shows a **Lyapunov function surface**, indicating system stability; the minimum point corresponds to the equilibrium where the system is most stable. and also shows a **curved bowl-like surface by the help of table (3, 4).**

Parameter	Value
π (Prey growth rate)	2.0
δ_1 (Carrying capacity of prey)	10.0
δ_2 (Allee threshold)	1.0
ξ_1 (Predation rate of predator on prey)	0.5
ξ_2 (Predation rate of super predator on prey)	0.4
ξ_3 (Predation rate of super predator on predator)	0.3
ψ_1 (Natural death rate of predator)	0.5
ψ_2 (Natural death rate of super predator)	0.6
$\mathbf{h_1}$ (Harvesting on predator)	0.01
$\mathbf{h_2}$ (Harvesting on super predator)	0.01
α (Herd shape parameter)	0.5 (circle shape)

Table 3: Parameter values used in the simulation.

Initial Condition	Value
$S(0)$ (Initial prey population)	5.0
$P(0)$ (Initial predator population)	2.0
$W(0)$ (Initial super predator population)	1.5

Table 4: Initial conditions for the simulation.

Simulation time: $\tau \in [0, 50]$.

Table 5: Parameter values and initial conditions for the preypredatorsuper predator model

Symbol	Description	Value
π	Growth rate of prey population	1.0
δ_1	Carrying capacity of prey	10
δ_2	Allee threshold for prey	1
ξ_1	Predation rate of predator on prey	0.5
ξ_2	Predation rate of super predator on prey	0.3
ξ_3	Predation rate of super predator on predator	0.2
ψ_1	Natural death rate of predator	0.1
ψ_2	Natural death rate of super predator	0.1
α	Herd shape parameter (circle shape)	0.5
q_1	Catchability coefficient for predator	0.05
q_2	Catchability coefficient for super predator	0.04
E_1	Harvesting effort on predator	0.8
E_2	Harvesting effort on super predator	0.6
$S(0)$	Initial prey population	4
$P(0)$	Initial predator population	2
$W(0)$	Initial super predator population	1

15. Conclusion

In this work, we introduced and examined a new fractional-order predatorpreysuper predator model that incorporates nonlinear harvesting, strong Allee effects, maturation delay, and herd behavior. By utilizing the Caputo fractional derivative, we captured the inherent memory effects of ecological systems, offering a more realistic portrayal compared to traditional integer-order models. The models formulation, featuring generalized functional responses and dual harvesting mechanisms, allowed for a thorough exploration of ecological dynamics under various biological and human influences.

Using rigorous analytical methods, we established the existence and local stability of equilibria and derived critical reproduction numbers that determine species survival or extinction. Additionally, we identified conditions where maturation delays can trigger Hopf bifurcations, leading to persistent oscillatory behavior. Extensive numerical simulations, performed via the AdamsBashforthMoulton method, supported our theoretical analysis and uncovered complex dynamical patterns, including stability switches and periodic solutions.

Overall, our findings enhance the understanding of multi-trophic ecological interactions shaped by memory, delay, and harvesting, providing valuable insights for ecological management and conservation. Future research could extend this model to incorporate stochastic influences, spatial variability, or adaptive harvesting strategies in memory-dependent ecological systems.

Conflict of Interest

The authors declare that there is no conflict of interest regarding the publication of this manuscript.

Acknowledgment

The authors express their sincere gratitude to Guru Ghasidas Vishwavidyalaya, Bilaspur, Chhattisgarh for providing the necessary resources and support for this research. Special thanks to our mentors and colleagues for their valuable insights and constructive discussions, which have significantly contributed to the development of this study.

Declaration

The authors confirm that the work presented in this paper is original and has not been submitted elsewhere for publication. All data, models, and code used in this study are available upon reasonable request.

Data Availability:

The data used in this study are available upon reasonable request.

Authors Contributions :

All authors have contributed significantly to the research, including conceptualization, mathematical modeling, analysis, and manuscript writing.

References:

[1] Angstmann, Christopher N., Bruce I. Henry, and Andrew V. McGann. "A fractional-order infectivity SIR model." *Physica A: Statistical Mechanics and its Applications* 452 (2016): 8693.

[2] Arif, Muhammad, Khaled Abodayeh, and Aftab Ejaz. "Stability analysis of fractional-order predatorprey system with consuming food resource." *Axioms* 12.1 (2023): 64.

[3] Bentout, Sidi, Samir Djilali, and Sunil Kumar. "Mathematical analysis of the influence of prey escaping from prey herd on three species fractional predator-prey interaction model." *Physica A* 572 (2021): 125840.

[4] Bhunia, Bivas, Laxman Bhutia, Tapas Kar, and Prasanta Debnath. "Explicit impacts of harvesting on a fractional-order delayed predatorprey model." *European Physical Journal Special Topics* 232 (2023): 26292644.

[5] Bhunia, Bivas, Tapas K. Kar, and Prasanta Debnath."Explicit impacts of harvesting on a delayed predatorprey system with Allee effect." *International Journal of Dynamics and Control* 12.2 (2024): 571585.

[6] Bi, Zhaoyang, Shuguang Liu, and Meng Ouyang."Spatial dynamics of a fractional predator-prey system with time delay and Allee effect." *Chaos, Solitons and Fractals* 162 (2022): 112434.

[7] Brahim, Ben, et al. "Effect of harvesting on a three-species predatorprey interaction with fractional derivative." *Fractals* 30.08 (2022): 2240234.

[8] Van den Driessche, Pauline, and James Watmough. "Reproduction numbers and sub-threshold endemic equilibria for compartmental models." *Mathematical Biosciences* 180.1-2 (2002): 2948.

[9] Diethelm, Kai. *The Analysis of Fractional Differential Equations: An Application-Oriented Exposition Using Differential Operators of Caputo Type*. Springer, 2010.

[10] Diethelm, Kai, Neville Ford, and Alan Freed."A predictorcorrector approach for the numerical solution of fractional differential equations." *Nonlinear Dynamics* 29.1 (2002): 322.

[11] Dwivedi, Ankita, and Verma, Santosh."Dynamical study of a fear-influenced fractional predator-prey model with disease spread." The European Physical Journal Plus 140.4 (2025): 306.

[12] Dwivedi, V. "Enhancing Pharmaceutical Supply Chains in Health Crises: Integrating Fuzzy Logic and Particle Swarm Optimization." Journal of Industrial Management and Optimization, vol. 21, no. 3, 2025, pp. 22112239.

[13] Ford, Neville, and Alistair Simpson. "The numerical solution of fractional differential equations: speed versus accuracy." *Numerical Algorithms* 26.4 (2001): 333346.

[14] Garrappa, Roberto."On linear stability of predictorcorrector algorithms for fractional differential equations." *International Journal of Computer Mathematics* 87.10 (2010): 21872203.

[15] Holling, C. S."Some characteristics of simple types of predation and parasitism." *The Canadian Entomologist* 91 (1959): 385398.

[16] Karthikeyan, S., P. Ramesh, and M. Sambath. "Stability analysis of harvested fractional-order prey-predator model with Holling type IV response." *International Journal of Nonlinear Analysis and Applications* 14.1 (2023): 20192030.

[17] Kilbas, Anatoly A., Hari M. Srivastava, and Juan J. Trujillo. *Theory and Applications of Fractional Differential Equations*. Elsevier, 2006.

[18] Kumar, G. R., et al."Dynamical study of fractional order Leslie-Gower model of predator-prey with fear, Allee effect, and inter-species rivalry." *Results in Control and Optimization* 14 (2024): 100403.

[19] Kumar, Sunil, Rajeev Singh, Rajendra Chauhan, and Neeraj Thakur."Investigation of an interacting fractional-order predatorprey system in presence of fear and harvesting." *Iranian Journal of Science* 47 (2023): 17391749.

[20] Lenzini, Francesco, and Jorge Rebaza."Non-constant predator harvesting on ratio-dependent predatorprey models." *Applied Mathematical Sciences* 4.8 (2010): 791803.

[21] Lubich, Christian.“Discretized fractional calculus.” *SIAM Journal on Mathematical Analysis* 17.3 (1986): 704719.

[22] Ma, Y., M. Zhao, and Y. Du.“Impact of the strong Allee effect in a predator-prey model.” *AIMS Mathematics* 7 (2022): 1629616314.

[23] Mandal, Manika, Shib Shankar Jana, Sarmishtha Nandi, and Tapas Kar. “Modeling and analysis of a fractional-order prey-predator system incorporating harvesting.” *Modeling Earth Systems and Environment* 7.2 (2021): 11591176.

[24] Martin, Calvin, and Shigui Ruan. “Predatorprey models with delay and prey harvesting.” *Journal of Mathematical Biology* 43.3 (2001): 247267.

[25] Miller, Kenneth S., and Bertram Ross. *An Introduction to the Fractional Calculus and Fractional Differential Equations*. Wiley, 1993.

[26] Mortuja, M. Golam, M. K. Chaube, and Sunil Kumar.“Dynamic analysis of a predator-prey system with nonlinear prey harvesting and square root functional response.” *Chaos, Solitons & Fractals* 148 (2021): 111071.

[27] Mukherjee, Manas, Debolina Pal, Supratik Mahato, and Emmanuel Bonyah.“Preypredator optimal harvesting mathematical model in the presence of toxic prey under interval uncertainty.” *Scientific African* 21 (2023): e01837.

[28] Nosrati, Kazem, and Masoud Shafiee. “Dynamic analysis of fractional-order singular Holling type-II predator-prey system.” *Applied Mathematics and Computation* 313 (2017): 159179.

[29] Owolabi, Kolade.“Computational study of noninteger order system of predation.” *Chaos* 29.1 (2019): 013120.

[30] Owolabi, Kolade.“Dynamical behaviour of fractional-order predator-prey system of Holling-type.” *Discrete and Continuous Dynamical Systems - Series S* 13.3 (2020): 823847.

[31] Paul, Subhasree, Ankit Mahata, Sayan Mukherjee, Prasanta C. Mali, and Biplab Roy.“Study of fractional order tri-trophic prey-predator model with fear effect on prey population.” *Advances in Pure Mathematics* 12.11 (2022): 652675.

[32] Podlubny, Igor. ”Fractional differential equations, volume 198 of.” Mathematics in Science and Engineering (1999): 7-35.

[33] Ramesh, K., et al. “Study on a fractional order delayed predatorprey model including prey refuge and type II functional response.” *Partial Differential Equations in Applied Mathematics* 8 (2023): 100555.

[34] Rihan, Faizal, H. Alsakaji, and C. Rajivganthi. “Stability and Hopf bifurcation of three-species preypredator system with time delays and Allee effect.” *Complexity* 2020 (2020): 115.

[35] Rihan, Faizal, S. Lakshmanan, A. Hashish, R. Rakkiyappan, and E. Ahmed.“Fractional-order delayed predator-prey systems with Holling type-II functional response.” *Nonlinear Dynamics* 80 (2015): 777789.

[36] Rosenzweig, Michael, and Robert MacArthur. “Graphical representation and stability conditions of predatorprey interactions.” *The American Naturalist* 97 (1963): 209235.

[37] Sarkar, Kankan, and Subhas Khajanchi. “An eco-epidemiological model with the impact of fear.” Chaos: An Interdisciplinary Journal of Nonlinear Science 32.8 (2022).

[38] Wang, Qing, and Rui Han. “Dynamics of fractional order predatorprey models with refuge and Allee effect in prey: with and without time delay.” *Qualitative Theory of Dynamical Systems* 24 (2024): 49.

[39] Yavuz, Mehmet, and Nihal Sene. “Stability analysis and numerical computation of the fractional predatorprey model with the harvesting rate.” *Fractal and Fractional* 4.3 (2020): 35.

[40] Zhang, Xiaoxue, Xiaojing Xu, and Min Liu.“Global Hopf bifurcation and positive periodic solutions of a delayed diffusive predatorprey model with weak Allee effect for predator.” *Advances in Continuous and Discrete Models* 2025 (2025): Article 19.